1998

Effects of physical and chemical properties of bright and dull coal lithotypes on the formation of char particles

Chad G. Tomforde
University of North Dakota

EFFECTS OF PHYSICAL AND CHEMICAL PROPERTIES OF BRIGHT AND DULL COAL LITHOTYPES ON THE FORMATION OF CHAR PARTICLES

by

Chad G. Tomforde
Bachelor of Science, Bridgewater State College, 1995

A Thesis

Submitted to the Graduate Faculty

of the

University of North Dakota

in partial fulfillment of the requirements

for the degree of

Master of Science

Grand Forks, North Dakota
May
1998

This thesis, submitted by Chad G. Tomforde in partial fulfillment of the requirements for the Degree of Master of Science from the University of North Dakota, has been read by the Faculty Advisory Committee under whom the work has been done and is hereby approved.

(Chairperson)

4/17/98

This thesis meets the standards for appearance, conforms to the style and format requirements of the Graduate School of the University of North Dakota, and is hereby approved.

Dean of the Graduate School

4-21-98

Date

PERMISSION

Title Effects of Physical and Chemical Properties of Bright and Dull Coal Lithotypes on the Formation of Char Particles

Department Geology and Geological Engineering

Degree Master of Science

In presenting this thesis in partial fulfillment of the requirements for a graduate degree from the University of North Dakota, I agree that the library of this University shall make it freely available for inspection. I further agree that permission for extensive copying for scholarly purposes may be granted by the professor who supervised my thesis work or, in his absence, by the chairperson of the department or the dean of the Graduate School. It is understood that any copying or publication or other use of this thesis or part thereof for financial gain shall not be allowed without my written permission. It is also understood that due recognition shall be given to me and to the University of North Dakota in any scholarly use which may be made of any material in my thesis.

Signature Chad G. Tomford

Date 4/19/98

TABLE OF CONTENTS

LIST OF ILLUSTRATIONS

LIST OF TABLES

ACKNOWLEDGMENTS

I would like to express my sincere appreciation to the University of North Dakota-Energy and Environmental Research Center for making this research possible. Specifically, I would like to thank Dr. Frank Karner, my advisor, and Dr. John Hurley for their guidance and helpful suggestions through out the course of this study. In addition, I would like to thank Dr. Nels Forsman for providing his time and helpful comments.

I would also like to thank the numerous people that provided their time and assistance during this study. I would like to thank Mr. James J. McCaffrey, the superintendent of Enlow Fork Coal Mine for allowing me to sample bituminous coal for this project. I also would like to show grateful appreciation to Mr. James Goss at Eagle Butte Coal Mine for his time, helpful comments, and assistance in the collection of subbituminous coal. I would also like to thank the staff at the Energy and Environmental Research Center, Oak Ridge National Laboratories, and the Anatomy Department at University of North Dakota for their analytical support.

Most importantly, I would like to thank my family for their support and love. I would also like to express my utmost appreciation to my best friend Bethany Bolles for her continuous assistance and support during my endeavors.

ABSTRACT

The Energy and Environmental Research Center is working with EPRI and a consortium of companies in partnership with DOE to determine factors causing sticky ash to blind or bridge hot-gas cleanup filters. In this study, bright and dull lithotypes were separated from bituminous, subbituminous and lignitic coals to determine physical and chemical properties that may lead to the formation of different charforms, and consequently, fine and sticky ash that is problematic in coal-fired combustion systems.

Proximate and ultimate, maceral, and energy dispersive X-ray fluorescence (EDXRF) analyses were used to characterize each lithotype. A bench-scale pressurized fluidized-bed reactor (PFBR) was used to produce ash and char from the lithotypes. The lithotypes and char were examined with transmission electron microscopy. Nanometer-scale inorganic inclusions found in the char were investigated with energy dispersive spectroscopy. Char morphology and abundance were determined by scanning electron microscopy using image point-counting techniques.

PFBR tests and electron microscopy show that lithotype reactivity controls char morphologies, does not influence ash liberation in fluidized bed combustors, but may have an effect in other types of combustion. In addition, nanometer-scale inclusions observed in the subbituminous bright lithotype may affect fine

ash formation in coal-fired combustion systems. Bright and dull lithotypes are similar with respect to the results of proximate and ultimate analyses except ash. The dull lignite, subbituminous, and bituminous lithotypes contain 9.39, 10.29, and 3.74 weight percent ash. The lignite, subbituminous, and bituminous bright lithotypes contain 3.90, 4.80, and 3.33 percent ash. EDXRF analyses show that the ash obtained from dull lithotypes contains more silicon whereas the ash associated with the bright lithotypes has more calcium, magnesium, sodium, and sulfur. Maceral analyses show that the bright lithotypes separated from lignite, subbituminous, and bituminous coals contain 97%, 97%, and 89% reactive macerals. Dull lithotypes of lignite, subbituminous, and bituminous coals have 74%, 89%, and 66% reactive macerals. The principal charforms identified are cenosphere, honeycomb, and solid. Bituminous bright lithotypes produce thin-walled cenosphere and thin-walled honeycomb charforms. Dull lithotypes produce thick-walled cenospheres, honeycomb char particles, and solid fragments. Subbituminous bright lithotypes produce abundant thin-walled honeycomb charforms. Less reactive charforms are associated with dull samples. High contrast nanometer-scale inclusions found in the subbituminous bright lithotype may influence the formation of fine and sticky ash. The PFBR tests show that the effect of lithotype on the quantity of fine ash formation in the PFBR is negligible. However, the lithotypes differ in char morphology, which is related to original maceral content.

CHAPTER I

INTRODUCTION

Purpose

Coal is used for numerous industrial activities including steel production; heating and powering foundries and cement plants; production of linoleum, detergents, perfumes, fungicides, insecticides, solvents, and wood preservatives; and gas, primarily methane. Most importantly, coal is used to generate nearly 56% of this country's electricity, because it occurs more abundantly than other fuels, and is a cost-effective fuel source for generating inexpensive and dependable electric power (Chircop, 1996).

The ash that results after total combustion of coal is of particular environmental concern, and has strong implications on the utilization of coal in industry. Ash that passes through the combustion system is released into the atmosphere as fine particulate matter. The mineral matter that forms during coal-combustion may be sticky and adhere to the walls of conventional furnaces creating a heat insulate that may cause thermal mechanical failure or chemical degradation of high temperature filters (Sawyer et. al., 1990). These problems associated with fly-ash in coal-fired boilers can cause electric utility plants to shutdown, an expense that may cost $100,000 per day (DOE, 1981). The stickiness of the ash is dependent on the size and composition distributions of

the ash particles which in turn are dependent on the physical and chemical properties of the coal and char. A complete characterization of different lithotypes from bituminous, subbituminous, and lignitic coals, and of their associated char particles is necessary to determine importance in causing hot-gas cleanup filters to be blinded and to malfunction because of ash buildup.

Objectives

The size distribution and compositional variation of ash particles formed during coal combustion depend on the occurrence of the inorganic components in coal. In addition, maceral content may play a major role in ash characteristics. This project examines how natural assemblages of macerals, lithotypes, influences combustion.

Organic microstructures concentrated in certain macerals may affect nanometer-scale inorganic particles in coal. The organic microstructures are affected by the original plant matter and coalification processes, and may contain voids that are filled by the precipitation of nanometer-scale inorganic components. A molecular cage formed by a unique arrangement of hexagonal and pentagonal carbon rings is one example of an organic microstructure that may exist in coal (Bailey, 1995). Relatively small inorganic molecules may precipitate within the cages during coalification processes. Figure 1 shows a buckminsterfullerene ('buckyball'), C_{60}, that may be present in coal which may be filled with nanometer-scale inorganic grains. Small inorganic inclusions may

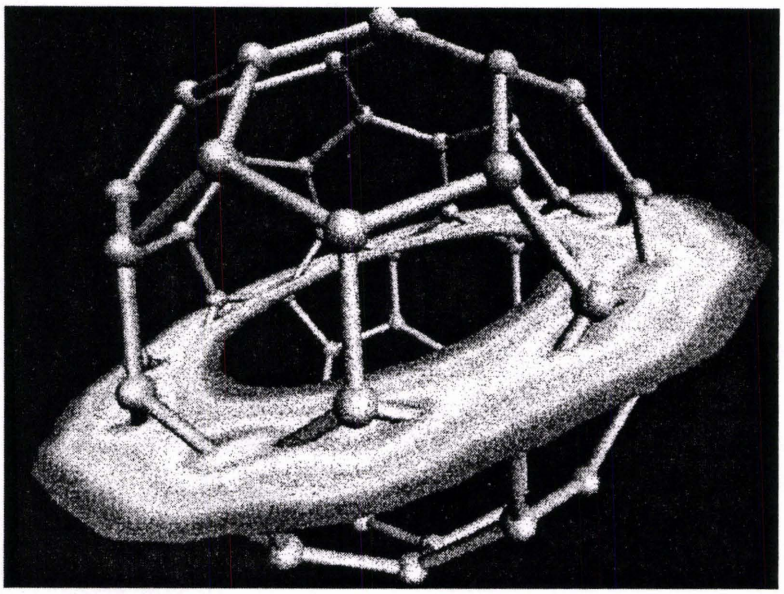

Figure 1. An example of an organic microstructure that may exist in coal (Bailey and Bailey, 1995) that may contain nanometer-scale inorganic particles. Specifically, this is the chemical structure of buckminsterfullerene, C_{60}, showing its electron density on the equatorial plane.

precipitate in nanometer-scale pores existing in macerals. Harris and Yust (1976) found spherical particles approximately 25 nanometers in diameter in pores within liptinite macerals. However, their chemical identity was not determined. One objective of this study is to determine if there are certain mineral types and sizes, specifically nanometer-scale inorganic inclusions that are enriched in bright and dull coal lithotypes and char.

Some macerals are more reactive than others, and will produce porous or vesicular charforms after partial combustion. Less reactive macerals may produce dense charforms. Figure 2 illustrates porous and dense charforms. During combustion, dense charforms may shed fine ash particles that produce a sticky cake on hot-gas cleanup filters. If miscible, fine ash that adheres to the surface of porous char may coalesce to form one larger ash particle. In a combustion system, this will produce coarser ash that is easier to remove than fine ash. A second objective of this study is to determine char morphologies and abundance produced by the different lithotypes that may cause the formation of fine and sticky ash.

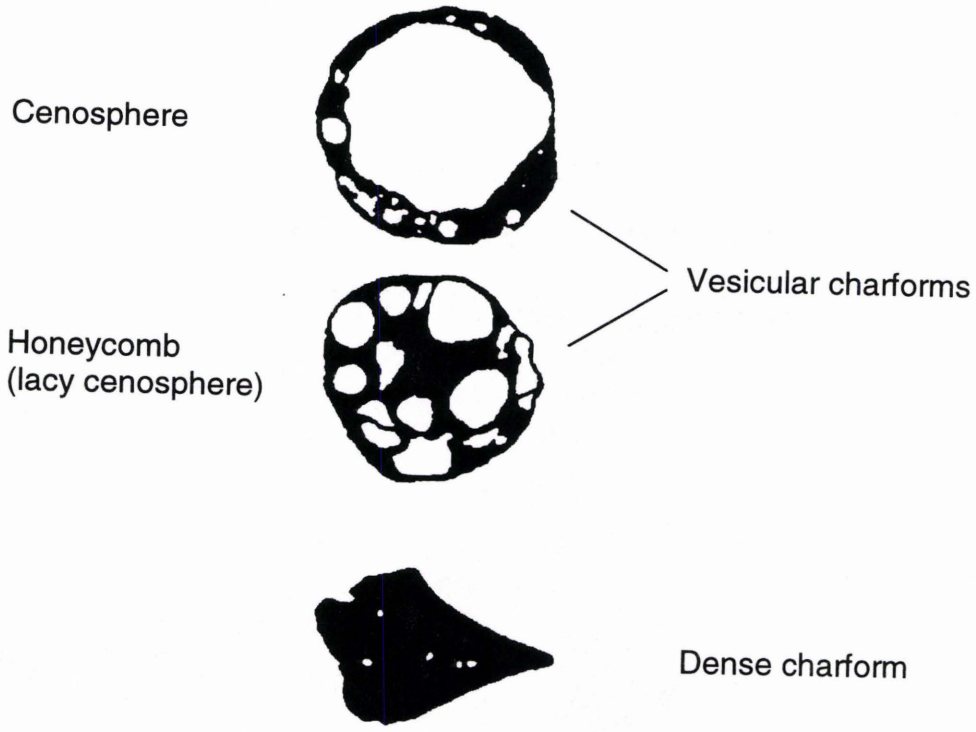

Figure 2. Vesicular and dense charforms produced by partial combustion of different coal lithotypes (modified after Alverez et al., 1997).

CHAPTER II

BACKGROUND AND PREVIOUS STUDIES

Coal Lithotypes and Macerals

Nomenclature

Macerals are the microscopically distinguishable organic components of coal, but including any mineral matter not discernible under the optical microscope (ASTM, 1995). They are coalified plant remains whose form and structure are preserved (Teichmueller, 1982). Coal lithotypes are the visible distinct layers in a 'banded' coal seam that are characteristic assemblages of macerals. The term 'band' implies two dimensions, whereas 'band' in a coal seam has three dimensions. The terms coal 'layer' or 'lens' will be used instead of 'band'. Coal layers can be separated by differences in color, brightness, composition, and texture. Most coal layers are lenticular and could be called coal lenses. For example, vitrinite macerals originate from woody material that are deposited in a coal swamp or peat bog that form discontinuous bright layers or lenses in a coal seam after burial and coalification. Specific assemblages of macerals, and to some extent, abundance of inorganic components determine the different lithotypes.

Lithotypes

Two systems for classifying lithotypes are common. Stopes (1919)

introduced the terms vitrain, clarain, durain, and fusain to characterize the different megascopic layers in coal. Thiessen and Francis (1929) proposed the terms anthraxylon and attritus for bright and dull layers in a given coal seam. The classification presented by Stopes (1919) is the common system used by coal scientists.

Vitrain layers are relatively narrow, vitreous, and uniformly thick. Ideally, brilliant vitrain layers are between 2 to 8 mm thick and break conchoidally or into cubes. Clarain essentially occurs as thin, alternating layers of durain and vitrain. Clarain is variable in thickness and has a smooth and shiny surface when broken at right angles to the bedding plane. Durain layers are dull, hard, and have a lumpy surface when broken. They typically have variable thickness. Fusain occurs as patches and wedges of powdery and fibrous strands. It occurs as very thin layers that can be easily scraped off the surface of other lithotypes. They are shiny or dull depending upon the angle of incident light. The lithotypes of Stopes' classification have subunits called microlithotypes which consist of layers at least 50 microns in thickness (Stach, 1982). The lithotypes and microlithotypes are described in Table 1.

Hower and Esterle (1989) present a logical and useful scheme for the classification of coal lithotypes. Their system clearly shows the association between lithotype and maceral. The lithotype analysis used in this study follows Hower's and Esterle's representation (Table 2).

Table 1. Summary of microlithotypes and lithotypes for subbituminous and bituminous coals (after Stach, 1982).

Microlithotype Group	Maceral Group Composition
Vitrite	Vitrinite > 95%
Liptite	Liptinite > 95%
Inertite	Inertinite > 95%
Clarite	Vitrinite + Liptinite > 95%
Vitriniertite	Vitrinite + Inertinite > 95%
Durite	Inertinite + Liptinite > 95%
Trimacerite	Vitrinite > Inertinite and Liptinite; Liptinite > Inertinite and Vitrinite; or Inertinite > Vitrinite and Liptinite
Lithotype	**Microlithotype Group Composition**
Vitrain	Vitrite and Clarite
Clarain	Vitrite, Clarite, Durite, Trimacerite and Fusite
Durain	Durite and Trimacerite
Fusain	Fusite

Table 2. Lithotypes of humic coals and some representative properties in high volatile bituminous Kentucky coals (slightly modified after Hower and Esterle, 1989). This scheme shows the association between lithotype and maceral which is useful in classifying lithotypes in the field.

Lithotype	Layers (% bright)	No. Samples	Group Macerals (mean)		
			Vitrinite	inertinite	liptinite
vitrain	>90				
bright clarain	65-90	93	85.6	7.8	4.4
clarain	35-65	73	79.9	9.8	4.1
dull clarain	10-35	30	71.1	15.8	8.6
durain	<10	42	42.5	34.9	16.4
fusain	fibrous; silky luster				

Macerals

The three maceral groups comprising subbituminous and bituminous coals are vitrinite, liptinite (exinite), and inertinite. Huminite macerals of the lignitic coals have the same plant precursors of the vitrinite macerals of the subbituminous and bituminous coals. The degree of coalification controls the formation of vitrinite or huminite macerals. These processes will be discussed further in the section dealing with coalification. It is the different assemblages of these macerals that define a particular coal microlithotype. Different combinations of these microlithotypes govern the formation of a certain lithotype.

In general, the vitrinite macerals originate from woody material such as roots, bark, and branches. The degradation of lignin and cellulose of woody cell walls forms humic substances, which then may oxidize through the process of 'humification' to form humic acids. Humic acids may undergo a process termed 'gelification', which forms huminite and subsequently the vitrinite macerals. These processes fall under the categories 'peatification' and 'coalification', which will be discussed in more detail in the coalification section in this paper. The liptinite group contains macerals originating from spores, cuticles, resins, and algae. The inertinite macerals are derived by 'fusinitization' of woody cell walls. Fusinitization is caused by charring, oxidation, and fungal degradation before deposition or on the peat surface (Teichmueller, 1982). The origins of the macerals of each group are summarized in Tables 3 and 4.

Table 3. Summary of the macerals of subbituminous and bituminous coals (after Stach, 1982 and ASTM, 1995).

Group Maceral	Maceral	Origin
Vitrinite	Telinite	Cell walls of woody material from trunks, branches, stems, leaves and roots. Commonly filled with collinite.
	Collinite	Structureless constituent of vitrinite originating from humic gel that frequently fills telinite.
	Vitrodetrinite	Detritus fragments of telinite and collinite.
Liptinite	Sporinite	Spores and Pollens.
	Cutinite	Cuticles from leaves, stems, needles, shoots, and stalks.
	Resinite	Resins and oils from plants.
	Alginite	Algae.
	Liptodetrinite	Detritus fragments of sporinite, cutinite, resinite, and alginite.
Inertinite	Micrinite	Fine grained organic detritus. Occurs as round, nearly 1 micron in diameter grains.
	Macrinite	Uncertain, but probably fusinized collinite. Occurs as 'groundmass' where other macerals may be embedded in it.
	Fusinite	Carbonization or charring of the same plant precursors of vitrinite macerals.
	Semifusinite	Partially charred plant plant precursors of the vitrinite macerals.
	Sclerotinite	Fungal remains and fusinitized resinites or collinites.
	Inertodetrinite	Uncertain, because it occurs as fragments less than 30 microns of fusinite, semifusinite, macrinite and sclerotinite.

Table 4. Summary of the macerals comprising lignitic coals (after ICCP, 1971).

Group Maceral	Maceral Subgroup	Maceral	Origin
Huminite	Humotelinite	Textinite	Cell walls originated from woody precursors; ungelified.
		Ulminite	Woody tissue that is partly gelified.
	Humocollinite	Gelinite	Completely gelified plant residues that fill cell walls.
		Corpohuminite	Tannin-rich cell excretions that fill cork and bark cells.
	Humodetinite	Attrinite	Detrital, ungelified, humic material; occurs as 'groundmass'.
		Desinite	Gelified attrinite.
Liptinite		Sporinite	Spores and Pollens.
		Cutinite	Cuticles from leaves, stems, needles, shoots, and stalks.
		Resinite	Resins from plants.
		Suberinite	Cell walls of woody plants that have been corkified.
		Alginite	Algae.
		Liptodetrinite	Detrital fragments of other liptinite macerals.
		Chlorophyllinite	Chlorophyl from leaves, stems, and fruits.
Inertinite		Macrinite	Uncertain, but probably fusintized humocollinite.
		Fusinite	Charring of the same plant precursors of huminite macerals.
		Semifusinite	Partial charring of the precursors of the huminite macerals.
		Sclerotinite	Fungal remains and fusinitized resinites or collinites.
		Inertodetrinite	Uncertain, but probably detrital fragments of the other inertinite macerals.

Chemistry

Maceral chemistry influences the formation of porous and dense char particles. The origin and the chemistry of each maceral group are functions of the original plant material, initial decomposition of the plant material at the peat stage, and the degree of coalification. The three maceral groups have different chemistry. Macerals belonging to a particular group have similar chemistry and reflectance, but differ in morphology and structure. The chemical compositions of the maceral groups are developed by the biochemistry of the original plant material, and then by coalification processes. Their chemical properties gradually become equivalent with increasing rank, until they become essentially identical at the meta-anthracite stage.

The vitrinite macerals are composed of various humins that consist of aromatic nuclei with aliphatic organic groups attached to them (Stach, 1982). The organic components of vitrinite become more aromatic with increasing rank. For example, as coalification proceeds, bonds between the aromatic portions and aliphatic functional groups such as hydroxyl, carboxylic acid, and methyl groups break, releasing the aliphatic hydrocarbons as gas. A possible mechanism for the loss of these functional groups with increasing coalification is dehydration, followed successively by decarboxylation and demethanation (Van Krevelen, 1981).

The liptinite macerals have the highest hydrogen content of all the macerals. Their chemical compositions closely resemble the chemistry of their plant precursors: sporine, cutine, resins, waxes, and algae. These macerals are also characterized by having a high aliphatic fraction, therefore containing more volatile matter than the other two maceral groups. They become difficult to discern at the mid-volatile bituminous and anthracite stages, because their reflectance closely resembles that of the vitrinite macerals. In addition, physical characteristics are absent at higher ranks.

The inertinite macerals have similar chemistry to the vitrinite macerals with one main exception; they have undergone some previous dehydrogenation (Van Krevelen, 1981). These macerals commonly have low hydrogen content, high carbon content, and a higher aromatic content than vitrinites. Refer to Stach, 1982 and Van Krevelen, 1981 for a complete review on the chemistry of the three maceral groups.

In 1957, Dormans, Huntjens and Van Krevelen determined that when macerals from the same rank coal are compared, the following chemical characteristics can be assumed: for hydrogen content, liptinite > vitrinite > inertinite; for oxygen content, inertinite > vitrinite > liptinite; and for carbon content, inertinite >vitrinite >liptinite (Van Krevelen, 1981). As rank increases for a particular coal as shown by an increase in carbon content, the oxygen content of the macerals decrease until the macerals have nearly identical oxygen and

carbon contents, somewhere near 95% carbon. The hydrogen content of liptinites decreases with increasing carbon content, while the hydrogen content of the vitrinites and inertinites somewhat increase to the mid-volatile bituminous stage, then decrease with increasing carbon content. Van Krevelen presented these general chemical characteristics for the different macerals with atomic H/C and O/C diagrams (Van Krevelen, 1981, figs. VI, 1-5).

When coal particles enriched in macerals of the liptinite and vitrinite groups are burned at a rapid rate they begin to melt and experience properties of plasticity. This is commonly known as the thermal plastic phase. Coal particles that experience thermal plasticity consist of macerals with relatively high hydrogen content and relatively low oxygen content. During and after the thermal plastic phase organic bonds in the coal particles break, releasing functional groups as gas (pyrolysis). Coal particles that experience thermal plasticity are termed 'reactive', where as coal particles that do not pass through this phase are termed 'inert'. Reactive coal particles should produce char particles with high void to solid ratio, and inert coal particles should produce char with lower void to solid ratio. In order of decreasing reactivity, macerals of the same rank can be listed as liptinite, vitrinite, and inertinite. This order is largely a function of the chemistry of the macerals.

Coalification

Coalification is the progressive maturation of peat through the stages of lignite, subbituminous and bituminous coals to anthracites and meta-anthracites (Teichmueller, 1982 and Gerencher, 1983). A coal's rank, and to some degree its chemistry is affected by coalification processes. Properties such as reflectance, calorific value, volatile matter, moisture content, carbon content, and hydrogen content are controlled by the degree of coalification. These properties affect how coal burns, and the physical and chemical properties of the intermediate phase char, and subsequently the fly-ash after complete combustion. Refer to Francis (1961), Van Krevelen (1981), Teichmueller and Teichmueller (1966, 1967, 1968, 1982), Stach (1982), Given (1984), Stout and Spackman (1987), and Gerencher (1983) for a more intensive discussion of coalification processes. Two stages of coalification are generally recognized; biochemical and geochemical.

Biochemical Coalification

Biochemical coalification is the first process that significantly affects the composition of coal, and for this reason a short discussion on this subject will follow.

Biochemical coalification, which incorporates peatification, is the biogenetic alteration of plant materials through the stages of peat and lignite (Gerencher, 1983, Francis, 1961, Van Krevelen, 1981, and Teichmueller, 1982).

It can be referred to as diagenesis. Moisture content decreases and carbon content increases during this phase. Humification and gelification are the main processes of biochemical coalification. Humification is the chemical and physical degradation of plant matter by oxidation reactions controlled by microorganisms (Teichmueller, 1982). This phase of coalification produces humic material at the peat stage. During gelification, the humic material is brought into a colloidal solution that, later, desiccates into a gel.

Stout and Spackman (1987) propose that the process of humification is divided into two main processes: alteration and degradation of cell walls. In alteration, the cell walls of woody material stay intact, but microorganisms chemically alter the cell wall polymers. In degradation, the cell walls lose their structural integrity. The biogenetic alteration of plant material to humic substances can be described entirely by the term 'humification', since there is evidence that alteration and degradation occur simultaneously.

Geochemical Coalification

Geochemical coalification, also known as coal metamorphism, is the process that sequentially transforms lignite through the stages of subbituminous and bituminous coals, to anthracites and meta-anthracites. Huminite macerals of lignite transform into vitrinite of the subbituminous, bituminous and anthracite coals during geochemical coalification. This pseudomorphologic transformation is commonly called 'vitrinitization' (Teichmueller, 1982). During early stages of

geochemical coalification, organic material in the subsiding coal bed is compressed by overburden pressure. This results in a decrease in oxygen content, moisture content, and porosity, while carbon content, calorific value, and optical anisotropy increase. Pressure has a minimal effect on the coal bed in late stages of geochemical coalification, while, on the other hand heat is the controlling factor (Teichmueller and Teichmueller, 1968). In fact, pressure may retard chemical reactions during the later stages of coal metamorphism (Teichmueller, 1982).

The pioneering work by Teichmueller and Teichmueller (1968) showed that high temperatures needed for coalification result from deep burial of the coal bed. Their study strongly suggested for the first time that hydrogen content and moisture content decrease, and carbon content and calorific value increase with burial. Teichmueller and Teichmueller (1968) determined that time and geothermal gradient are the most important factors affecting coal metamorphism. The same rank coal can form at low temperatures over a long time interval, or at high temperatures during a short time interval. Temperatures must be greater than 100° Celsius for the development of bituminous coals, regardless of the period of time it is subjected to that temperature (Teichmueller and Teichmueller, 1968). An increase in heat by contact metamorphism also affects the rank of coal (Teichmueller and Teichmueller, 1968).

Coal Rank

The degree of metamorphism is measured by coal rank, and is the extent to which the organic plant material has been chemically and physically altered along the pathway through lignite, subbituminous and bituminous coals to anthracites and meta-anthracites (Given, 1984). Coalification processes strongly influence changes in the chemistry of the huminite and vitrinite macerals. Most previous work suggests that vitrinite macerals become more aromatic and less aliphatic, and aromatic rings show increasing condensation with increase in rank (Van Krevelen, 1981; Given, 1984; Stach, 1982; and Gerencher, 1983).

Liptinite macerals resist physiochemical alterations at the early stages of coalification, but experience abrupt change at what is referred to as 'coalification jumps' (Gerencher, 1983). The first coalification jump occurs at the high volatile bituminous stage where bitumens are formed from liptinite and vitrinite macerals. The second coalification jump corresponds to the transition from high-volatile to mid-volatile bituminous coal. Bitumins formed from the first jump break into hydrocarbons of smaller molecular size (Teichmueller and Teichmueller, 1982). Reflectance of the liptinite and vitrinite macerals increases dramatically during the coalification jumps. These two macerals become increasingly more difficult to distinguish as the rank increases.

The inertinite macerals experience the smallest amount of change during coalification. They become more aromatic with increase in rank, and lose what little hydrogen they have.

Coal Combustion

The physical and chemical transformations of coal particles during combustion include the evolution of inorganic species, and the development and burning of char. Together, these affect the reliability and efficiency of coal-fired combustion systems. The ash that forms during combustion can cause many problems such as; blinding and bridging of high temperature filters, the production of slag and deposits on combustion chamber walls, impedance of heat transfer, and erosion and corrosion of combustor components. The size distributions and chemical variations of the fly-ash govern these problems, which in turn are controlled by the occurrences of inorganic material in the coal. Formation of ash particles in boiler systems can cause costly interruptions in coal-fired utility plants.

In addition, char that forms during the combustion process can affect the dependability of coal-fired utility plants. Char is the combustible, carbon-rich solid produced as a result of partial combustion of coal. The formation of char can be thought of as an intermediate phase affecting the characteristics of fly-ash. Ash particles <10 microns may be sticky and produce a coating on high temperature particulate filters that is difficult to remove (Dockter et al, 1997).

They may also escape to the environment if not removed from stack gasses (Helble and Sarofim, 1989). Physical factors responsible for the production of fine ash are (1) shedding of inorganic components from char particles and (2) char fragmentation during combustion. Char morphologies (charforms or chartypes) govern the degree of coalescence and shedding of ash particles as they appear on the surface of the char during combustion. This process affects the formation of fine and sticky ash in a coal-fired combustion system. The fragmentation of char during combustion also influences ash particle size distributions. Inorganic matter that appears on the surface of a char particle during combustion will coalesce to form one ash particle per char particle. This is usually not the case. Experimental results show that many ash particles form from single char particles due to char fragmentation (Helble and Sarofim, 1989). A third problem associated with char type is the production of unburned char found in fly-ash after complete combustion. Levels above 5% unburned char in fly-ash is undesirable for most power stations (Shibaoka, 1985). The unburned char is dependent on lithotype concentration, coal rank, particle size, and combustion properties.

Char

Char is the graphitic, hydrogen-deficient substance that remains after devolatization (pyrolysis). Coal particles with relatively high levels of hydrogen are more thermoplastic and will produce vesicular or porous char particles. Coal

particles with lower amounts of hydrogen are less thermoplastic and will produce dense char particles. The reactivity of the different charforms governs the efficiency of a coal-fired combustion system, and may also control the formation of fine and sticky ash.

Morphologies

Char morphologies are influenced by maceral variability in the coal, coal rank, occurrences of inorganic components, and combustion operating parameters, such as burning rates and particle sizes. The chief char morphologies are cenosphere, honeycomb, and unfused.

Three subclasses of the cenosphere charform are thin-walled, thick-walled, and lacy. These are commonly grouped as 'reactive' or vesicular char. McCollor et al. (1988) extended the terminology by introducing a more descriptive scheme for classifying different charforms produced by lignitic coal. The following description is after McCollor et al. (1988) except where noted. Cenospheres are described as having a high pore to solid ratio, and are composed of one to three main pores. Typically, they are round or umbrella shaped and contain nearly 90% void space. The formation of thin- or thick-walled cenospheres depends on a balance between the gas pressure generated within the particles and the surface tension, provided the particles experience a thermal plastic phase (Zheng and Zhijun, 1996). Lacy cenospheres contain many internal partitions (Lightman and Street, 1967), and may be equivalent to

mesospheres of McCollor et al. (1988). Mesospheres have more than three major pores and their walls are three to five times thicker than those in the cenosphere group. They generally have a subangular to round shape. The terms thin- and thick-walled lacy cenospere are used in this study instead of mesosphere. The honeycomb charform has a pore to solid ratio less than one, and is generally elongate and rectangular in shape. The pores are orientated subparallel to parallel to the short side of the particle, and the walls often contain secondary pores. The pores develop along the original bedding plane in inertinite-rich coal, or may be attributed to a mixture of reactive (vitrinite and low-reflectance inertinite) and unreactive (granular inertinite) zones in the coal particle (Zheng and Zhijun, 1996). During the devolatilization/plasticity phase in coal-combustion, the formation of vesicules within vitrinite may be restricted by inertinite producing a honeycomb char. Internal burning of solid char that leads to the production of elongated pores (Zheng et al., 1996) can also produce the honeycomb structure. Heterogeneous charforms containing irregular shaped pores and fragments of unfused or solid char are inertospheres. They are irregular shaped and are composed of approximately 30% void space. Unfused charforms are commonly angular in shape and contain few to no pores. They are sometimes called dense or solid char. They often contain cracks that resemble desiccation cracks, and commonly look similar to inertinite macerals.

Charforms closely resembling inertospheres and having greater than 30% mineral inclusions are termed mineral-rich.

Effects Controlling Char Morphologies and Reactivity

A fundamental question in char formation is what are the major factors that determine morphology, and consequently the production of fine ash and the rate of burnout in a combustion system. Effects of rank, maceral concentration, and operating parameters have been thoroughly investigated. Nearly all previous work is focused on char formation in some type of pulverized fuel combustion system, whereas very little research has been conducted using a fluidized-bed combustion system.

There has been some controversy in determining what factors have the greatest effect on the overall combustion process. Shibaoka et al. (1985) proclaim that coal rank plays the major role. First, they attempt to show that the duration of the different stages in combustion (induction, devolatilization / vesiculation, char combustion, and residual char combustion) all increase with increasing rank. Secondly, they provide a diagrammatic representation of morphological changes of vitrinite obtained from low and high rank coals that indicates differences during pulverized fuel combustion. To the contrary, Jones et al. (1985) maintain that maceral concentration is a controlling, but not overriding, factor in coal reactivity. Their results suggest that vitrinite macerals produce cenospheres, low-reflectance inertinite produce honeycomb

morphologies, and high-reflectance inertinite produce unfused charforms. The cenosphere charform shows obvious fluidity during pyrolysis, while honeycomb structures experience limited fluidity, and unfused charforms encounter no fluidity. There is evidence that the morphology of inertinite-derived char converges with vitrinite-derived char with increasing rank, shown by porosity decreases in the vitrinite-derived char (Jones et al., 1985).

In an attempt to clarify some of the ambiguities associated with the factors determining coal reactivity in pulverized fuel combustion, Pregermain (1988) studied the effects of rank, maceral concentrations, and particle size on burnout rates. He determined that a decrease in particle size from 100 to 80 microns to less than 50 microns leads to increased rate of burnout at lower temperatures for vitrinite-rich coal. This is due to an increase in surface area that consequently increases reactivity. Decrease in particle size for inertinite-rich coal has no effect on the reactivity, because the heterogeneous nature of inertinite macerals facilitate oxygen access to the core of the particle (Pregermain, 1988). Pregermain's (1988) conclusions are as follows: high rank inertinite-rich coal and high rank vitrinite-rich coal have nearly the same reaction rates during combustion; low rank vitrinite-rich coal burns faster than low rank inertinite-rich coal; and rank plays an important role, in that, high rank vitrinite-rich has lower reaction rates when burned than do low rank vitrinite-rich coal. In addition, maceral effects increase with decreasing particle size. In agreement with

Shibaoka (1985), Pregermain (1988) concludes that low-reflectance inertinite, such as semi-fusinite and inertodetrinite experiences thermal plasticity and burns as rapidly as vitrinite. High-reflectance inertinite, such as fusinite produces dense or unfused charforms.

Zheng and Zhijun (1996) show three main burning modes for different char types: constant-diameter, constant-density, and mixed. In constant-diameter burning, thin- and thick-walled cenospheres burn with a constant size and a decreasing density. As burning continues within secondary pores in thick-walled cenospheres and reactive areas in thin-walled cenospheres, density decreases while there is no change in diameter. Solid and fragment char burns in constant-density mode where the surface of the char reacts, resulting in decreased particle size. Due to loose structure in low rank coals, solid char may burn in a mixed-mode. Tunneling through the coal's primary bedding plane or micro-pores permits gases to penetrate to the interior of the particle. In conclusion, Zheng and Zhijun (1996) determined that coal rank and maceral variability controls charforms, hence reactivity, in pulverized fuel combustion.

Hamilton (1980) shows that the rate of heating during combustion is important to the development of vesicular and solid charforms. When the heating rate is slow (0.1 degrees Celsius/sec) plasticity does not occur for vitrinite separated from seven coals ranging in rank from lignite to anthracite. Plasticity does occur for the vitrinite samples when the heating rate is fast

(10,000 degrees Celsius/sec), and in fact, rank plays a minor role in the development of cenospheres at this rate of heating.

Inorganic Components

The inorganic components in coal exist as mineral grains and organically bound inorganic elements. Some common minerals found in coal are shown in Table 5. Minerals significant to the formation of a large proportion of ash are quartz, pyrite, gypsum, calcite, dolomite, kaolinite, illite, and montmorillonite (Hurley and Schobert, 1992). Previous work suggests that minerals dominate the inorganic components in high rank coals, and organically bound inorganic elements are more abundant in low rank coal (Kube et al., 1984 and Karner et al., 1994). There is a class of elements normally associated with inorganic compounds, while another class of elements is a basis for organic compounds. Elements commonly found in inorganic compounds, such as Na, Mg, Al, Si, K, Ca, Fe, and Ti, are referred to as inorganic elements. Some of these elements may be bound to organic compounds existing in coal, such as carboxylic groups (Kube et al., 1984). Specifically, they may be attached to salts formed by carboxylic acid. They can be referred to as organically-bound inorganic elements, organically-associated inorganic elements, cations associated with organic acid groups, or ion-exchangeable inorganic matter. The alkali and alkaline earth metals, specifically Ca, Mg, Na, and K are commonly organically-associated in low rank coal (Kube et al., 1984 and Karner et al., 1994).

Table 5. Common minerals existing in coal.

Kaolinite	$Al_2Si2O_5(OH)_4$
Illite	$(K,H_3O)(Al,Mg,Fe)_2(Si,Al)_4O_{10}[(OH)_2,H_2O]$
Muscovite	$KAl_2(Si_3Al)O_{10}(OH,F)_2$
Biotite	$K[Mg,Fe(II)]_3[Al,Fe(III)]Si_3O_{10}(OH,F)_2$
Orthoclase	$KAlSi_3O_8$
Albite	$NaAlSi_3O_8$
Calcite	$CaCO_3$
Dolomite	$CaMg(CO_3)_2$
Siderite	$FeCO_3$
Pyrite	FeS_2
Gypsum	$CaSO_4{\cdot}2H_2O$
Quartz	SiO_2
Hematite	Fe_2O_3
Magnetite	$Fe(II)Fe(III)O_4$
Rutile	TiO_2
Halite	NaCl
Sylvite	KCl

The inorganic components in coal experience complex physical and chemical transformations during combustion. Decomposition, fragmentation, coalescence, vaporization, and condensation are several processes affecting discrete mineral components in combustion (Hurley and Schobert, 1992). The organically-associated inorganic elements may vaporize and, then, condense on the surface of char particles and on combustion system components. The organically-bound inorganic elements that may be dispersed within the macerals of low rank coal (Kube et al., 1984 and Karner et al., 1994) might strongly influence the stickiness of ash deposits on high temperature ceramic filters.

Nanometer-Scale Inclusions

A transmission electron microscopy study carried out by Hurley and Schobert (1992) revealed the presence of high levels of nanometer-scale inorganic inclusions in subbituminous coal particles. The smallest size class observed is 2-3 nanometers (nm) in diameter. It was not possible to determine their chemical identity with energy dispersive spectroscopy, because of their extremely small size and confusion attributed to the high concentration of organically-associated inorganic elements present in the coal matrices. Therefore, it is not known if the nanometer-scale inclusions are, in fact, inorganic. It is possible that they are mesophase inclusions. Mesophase particles are liquid crystals that form during an intermediate phase in the conversion of vitrinite to coke by heating. Upon heating vitrinite obtained from

bituminous coal, Friel et al. (1980) determined the formation of dark, spherical, nanometer-scale inclusions. TEM micrographs presented by Friel et al. (1980) show a strong correlation between the appearance of nanometer-scale mesophase spheres and the nanometer-scale inclusions shown in Hurley (1990). However, Friel et al. (1980) observed nanometer-scale inclusions in vitrinite before heating. They suggest that bio-oxidation or a geothermal event may have produced enough heat to form mesophase spheres in the coal. In agreement with Hurley and Schobert (1992), minerals 2-3 nm were found in bituminous coal using scanning tunneling microscopy (STM) (Zareie et al., 1996). Their chemical identity was not determined, but their intense brightness as compared to the organic portion of the coal using STM imaging suggests that they are, indeed, inorganic. Spherical particles approximately 25 nm in diameter were found in pores occurring within liptinite macerals in two other studies (Harris and Yust, 1976 and 1981). The more recent study shows bands of nanometer sized minerals along bedding planes in vitrinite. Energy dispersive X-ray analysis and selected area diffraction data identified the spherical particles found in pores of liptinite macerals as the mineral aragonite ($CaCO_3$). The platy particles present along bedding planes of vitrinite appear to be kaolinite. A possible explanation proposed by Harris and Yust (1976) for the origin of the aragonite particles present in pores can be found in a separate study (Hennig, 1962) showing oxidation of graphite by colloidal-size metal particles causing the metal particles

to migrate along the surface creating a channel behind them. They suggest that the same processes may occur in coal until a pore captures the migrating particle.

Two ideas emerge for the formation of nanometer-scale inorganic components in coal; 1) they form within micro-pores in macerals and 2) they form within molecular cages present in coal.

Effects of Char and Inorganic Components on the Formation of Fine Ash

Transmission electron microscopy analyses on subbituminous coal and char (Hurley and Schobert, 1993) has shown two main morphological types of char particles; highly vesicular and dense char particles. The highly vesicular char particles contained more ash globules on the outer char surface than the dense char particles, but both char types had nearly the same amount of ash inclusions within their matrices. This suggests that coalescence of mineral components on the surface of the porous char is more apt to occur than on the surface of the dense char where the mineral material can be shed more easily. As devolatization occurs during combustion, gaseous jets of volatiles effusing from the char particle sets the particle in a high frequency rotation. Centrifugal forces created by the rotation of the char particle shed ash off the surface of the particle (Helble and Sarofim, 1989).

The fragmentation of char during combustion affects the size distribution of fly-ash. The reduction in size (comminution) of coal and char particles in a

fluidized-bed combustor was researched extensively by Chirone et al. (1991 and 1989). They show four principal modes of comminution: primary fragmentation, secondary fragmentation, fragmentation by uniform percolation, and attrition. Primary fragmentation occurs during devolatilization of coal particles. The weakening and breaking up of bridges that make up char particles cause secondary fragmentation. Fragmentation by uniform percolation occurs near the end of char combustion when the structure of the char particles suddenly collapses due to pore enlargement. Attrition is the abrasion of fine ash particles from char surfaces by collisions with the bed material and combustor components.

Fragmentation of char particles is largely controlled by char morphology. Baxter (1992) shows that char cenospheres produced by bituminous coal burn in a constant-diameter mode until they become brittle and friable and ultimately burst into many fragments. Solid and honeycomb char produced by lignite burn out in constant-density and mixed modes. These charforms did not fragment as readily as the porous char obtained from the bituminous coal, but instead formed ash droplets on their surfaces during combustion. The two coals produced similar amounts of fly-ash, but by two different proposed methods. As ash condensed on the surface of dense char, it was shed from the particle. On the other hand, porous char fragmented into many char particles, consequently producing fine fly-ash. Baxter (1992) did not acknowledge the effects of lithotype

or maceral content on the formation of porous and dense charforms. For a complete discussion on char fragmentation, see Baxter (1992 and 1990), Chirone et al. (1991 and 1989), and Helble and Sarofim (1989).

CHAPTER III

CHARACTERIZATION OF BITUMINOUS, SUBBITUMINOUS AND LIGNITIC COAL AND CHAR SAMPLES

Field and Megascopic Properties

The following discussion is a detailed description of the sampling and preparation methods used in the collection of bright and dull lithotypes from bituminous, subbituminous, and lignitic coals. This section also describes the different lithotypes separated from each coal. The purpose of this discussion is to aid subsequent researchers in the collection, separation, and description of coal lithotypes that may aid in physical and chemical characterization.

Pittsburgh #8 Bituminous Coal

Bituminous coal was collected from the Pittsburgh #8 coal bed, Enlow Fork Mine, West Finley, Pennsylvania. The Enlow Fork Mine is an underground coal mine that extracts nearly ten million tons of coal per year. Thirty percent of Pennsylvania's entire coal production is obtained from the Pittsburgh #8 coal seam (Edmunds, 1993). The coal was mined for steam, gas, and coke in the early to mid 1900's. Currently, it is mined almost exclusively for steam generating utility plants.

The Pittsburgh #8 coal averages 4 feet thick and extends over an area of 15,000 square kilometers in western Pennsylvania, eastern Ohio, northern West

Virginia, and the Maryland panhandle (Chyi et al., 1987). The coal bed was deposited in the north-northeast trending Dunkard basin of the Appalachian Province 295 million years ago (m.y.a) (Chyi et al., 1987). Clastic sediments accumulated in the Appalachian basin at the end of the Conemaugh Epoch of the Carboniferous Period. Growth of an extensive peat forming flora marks the beginning of the Monongahela Epoch, 290-330 m.y.a. (Stone, 1932). The Pittsburgh #8 coal is the lowest member of the Pittsburgh Formation and the Monongahela Group. Refer to Damberger (1974), Chyi (1987), and Cross (1971) for complete descriptions of the Pittsburgh coal.

Approximately 27 kg (60 lb.) of lithotype samples, 23 kg (50 lb.) of channel sample, and a lithologic section were collected from the underground mine. Figure 3 shows the major lithologic components of the Pittsburgh #8 coal seam. Portions of the coal seam that appeared predominantly bright or predominantly dull were targeted for the collection of lithotype samples. Ten pound bags were filled with bright and dull coal, and sealed to minimize contact with the atmosphere. The bags were labeled L1, L2, L3, and L5. Each sample was further concentrated into bright and dull coal in the laboratory. A geology hammer, putty knife, hack saw, heavy file, and a wire brush were used to separate the thin lithotype layers. The following discussion will characterize each sample megascopically based on weight percent bright coal, after Hower and Esterle (1989) (Table 2). For example, a lithotype containing 60% bright coal

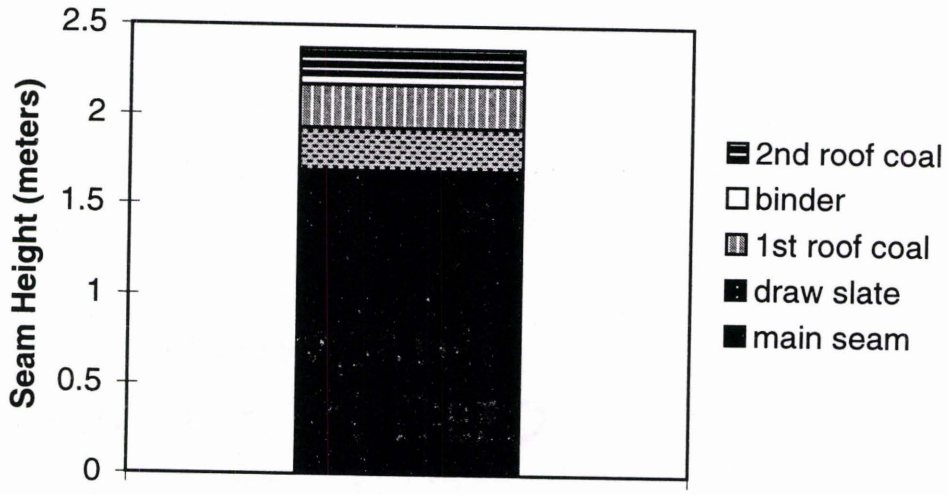

Figure 3. Cross section of the Pittsburgh #8 coal seam in the vicinity of lithotype sampling locations.

and 40% dull coal is described as bright (60%). A lithotype containing 90% dull layers and 10% bright is described as dull (10%).

Sample L1 was collected from the lower roof coal which represents bright coal in that section of the seam. This sample was separated into two bright subtypes, 4 kg bright (85%) and 1 kg bright (95%). The bright (85%) sample contains thin, hair-like, and wavy dull layers, and is classified as bright clarain. The bright (95%) sample is vitrain. Both subtypes are difficult to separate, because they crumble very easily, showing conchoidal fracture. The bright (85%) and the bright (95%) constitutes 80% and 20% of L1, respectively. These samples contain pyrite nodules and clay lenses.

Two bags labeled L2 were filled with ten pounds of coal collected from the middle of the main seam. Five subtypes were separated from the two bags: claystone, dull (5%), bright (60%), bright (90%), and bright (≈100%). The claystone ranged between one and 1.5 cm thick and comprises 3% of sample L2. The dull (5%) lithotype is typical durain and comprises 6% of L2. This lithotype occurs as thin layers, the thickest layer equal to 1 cm. The bright (60%) has many alternating, thin, dull and bright layers. It is typical clarain and makes up approximately 71% of sample L2. The bright (90%) has less thin dull layers associated with it and breaks easily into sharp rhombohedral pieces. This brittle subtype of L2 was difficult to separate from the rest of the coal. Nearly 18% of L2 is composed of this bright clarain. The bright (≈100%) is brilliantly bright,

crinkled in appearance, and softer than the bright (90%). This lithotype is present as layers 2-10 mm in thickness, and comprises approximately 2% of L2. This lustrous lithotype is typical vitrain.

Sample L3 was collected because it contained a high percent of dull coal. It was extracted from 24 cm below the clay parting in the main seam. Approximately 50% of the entire sample is dull. Three subtypes were separated from L3: dull (<10%), bright (60%), and bright (90%). The dull is a durain that contains few noticeable bright lenses. This lithotype is hard, gray, and breaks conchoidally. Approximately 26% of L3 contains this dull lithotype. Gradational changes between the two bright subtypes made separation and categorizing difficult. The bright (60%) makes up 71%, and the bright (90%) constitutes 7% of the sample. The bright (60%) separates more easily along bedding planes where very thin fusain layers are concentrated.

Sample L5 was collected from the bottom part of the main seam. There is a gradual transition from coal; to coal intermixed with claystone, to pure claystone near the floor of the main coal bed. Three subtypes were separated from this sample: dull (<10%), dull (50%), and bright (80%). The dull (<10%) comprise 30% of L5, and is quite different from the dull subtype in L3. The dullest subtype from L5 has claystone intermixed with it, giving it a grayish color, and making it dense and soft. This subtype was collected approximately 2 to 2.5 cm from the claystone floor. Sixty percent of L5 consists of dull (50%) which is

classed a clarain. Fusain layers do not occur as frequently in this subtype, as they do in the bright (60%) of L3. The bright (80%) subtype from L5 contains thin, hair-like dull layers, and some brilliant and crinkled bright layers. This lithotype makes up 10% of L5, and is classified as bright clarain.

The separated subtypes were mixed to produce lithotype sample standards for subsequent analytical tests. Four lithotype samples were fabricated; 1) super bright, 2) bright with pyrite, 3) bright and 4) dull. The super bright lithotype consists of; 1 kg bright (60%) from L3, 0.5 kg bright (90%) from L3, 0.2 kg bright (≈100%) from L2, and 1 kg bright (80%) from L5. The entire L1 sample (5 kg) was used to make the bright with pyrite lithotype sample. The bright lithotype sample was produced from 5 kg of bright (60%) separated from L2. The dull lithotype consists of 2 kg dull (<10%) taken from L3. These samples were crushed to pass a number eight mesh for chemical analyses. Figure 4 shows dull and bright portions in the bituminous coal.

Wyodak Subbituminous Coal

The Eagle Butte Mine in Gillette, Wyoming extracts subbituminous coal from two seams, together, known as the Wyodak coal bed. The Wyodak resides at the top of the Fort Union Formation, and was deposited 40-45 m.y.a. within the eastern flanks of the Powder River basin. The Powder River basin formed during the Laramide Orogeny where Cretaceous and early Tertiary rocks were folded into an asymmetric syncline (Glass, 1976). The upper bed was named

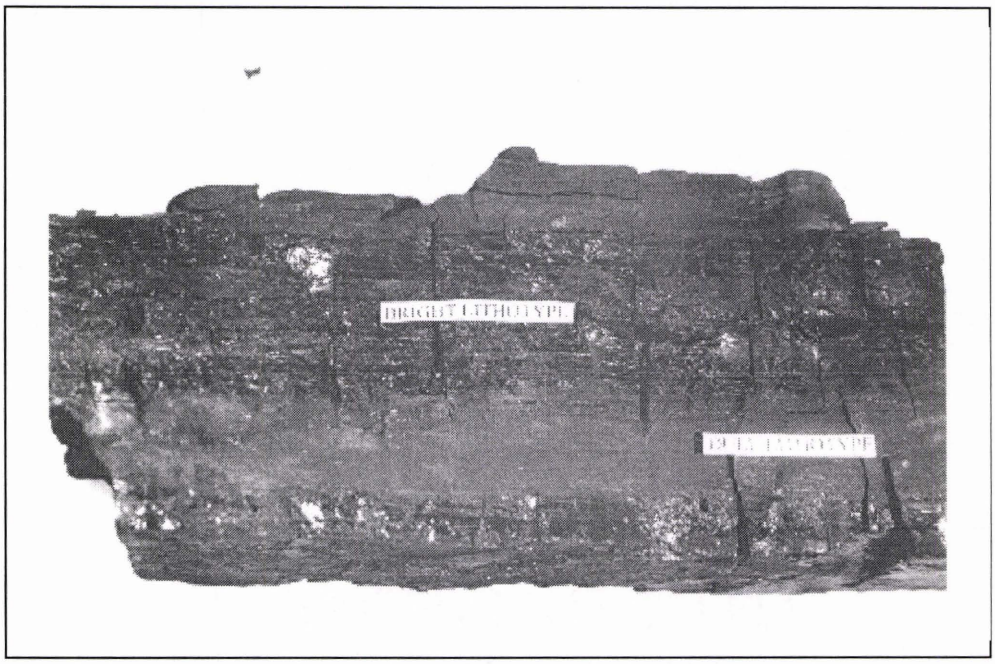

Figure 4. Bright and dull lithotypes in the Pittsburgh #8 bituminous coal.

the Roland coal bed, and the lower bed was named the Smith coal bed by Taff (1909) (Kent, 1986). They have also been correlated to the Anderson and Canyon coal beds. Recent work suggests that five coal beds merge eastward to form the Wyodak coal at Gillette, and Tongue River rocks above the Wyodak were removed by pre-Wasatch erosion (Kent, 1986). The Wyodak deposit is 97 kilometers long and 10-15 kilometers wide. The names 'Roland' and 'Smith' are still used for the coal mined at Eagle Butte Mine, because they were incorporated into the contracts written at the time the coal was leased from the U.S. Government and sold to prospective customers (Goss, 1996). The top of the 'Roland' seam lies beneath 30 to 200 feet of the Eocene Wasatch Formation. It averages 35 feet thick. A four foot carbonaceous claystone parting separates the 'Roland' from the 'Smith'. The 'Smith' coal is approximately 100 feet thick at Eagle Butte Mine, and is excavated in two lifts; the upper and lower.

Lithotypes in the Eagle Butte Coal are difficult to discern. Bright coal in the upper Smith has a swirly appearance that resembles tree ring structure. This type of coal, although not especially bright, originates from woody debris, and therefore, is assumed to have a high concentration of vitrinite. The dull coal is dirt black and contains white specks of mineral matter, presumably clay minerals. No swirly or tree ring appearance is noticeable in the dull. This coal breaks unevenly and seems blocky. The upper Smith also contains a dark black, fine

grained coal containing no noticeable structures. Shiny black patches within the matrix of this coal are probably vitrinite.

The lower Smith coal is similar to the upper Smith, although some differences were observed during the separation of bright and dull lithotypes. Vitreous bright coal exists as discontinuous layers within the dull coal. Very shiny and crinkled zones were found in the lower Smith. These are included with the bright samples. The dull coal appears gritty and friable. Fusain layers are included with the dull coal.

The Roland seam contains swirly bright coal and friable dull coal that is very similar to that of the Smith seam.

Three samples were collected from the Eagle Butte Mine; 16 kg from the Roland seam, 16 kg from the upper Smith seam, and 14 kg from the lower Smith seam. Bright (90%), dull (10%), and mixed (20%) lithotype samples were prepared for analytical tests. The mixed lithotype does not seem to be purely a mixture of bright and dull layers, but also has a different texture. Maceral analysis confirms that the sample is a different lithotype. Bright and dull lithotypes in the subbituminous coal are represented in Figure 5.

Beulah-Zap Lignite

Lignite was sampled from pit # 62, east mine area of the Beulah-Zap coal bed at the Freedom Mine, Beulah, North Dakota. The Beulah-Zap averages 3.5 m and merges with the Spaer bed north of Beulah making the combined coal

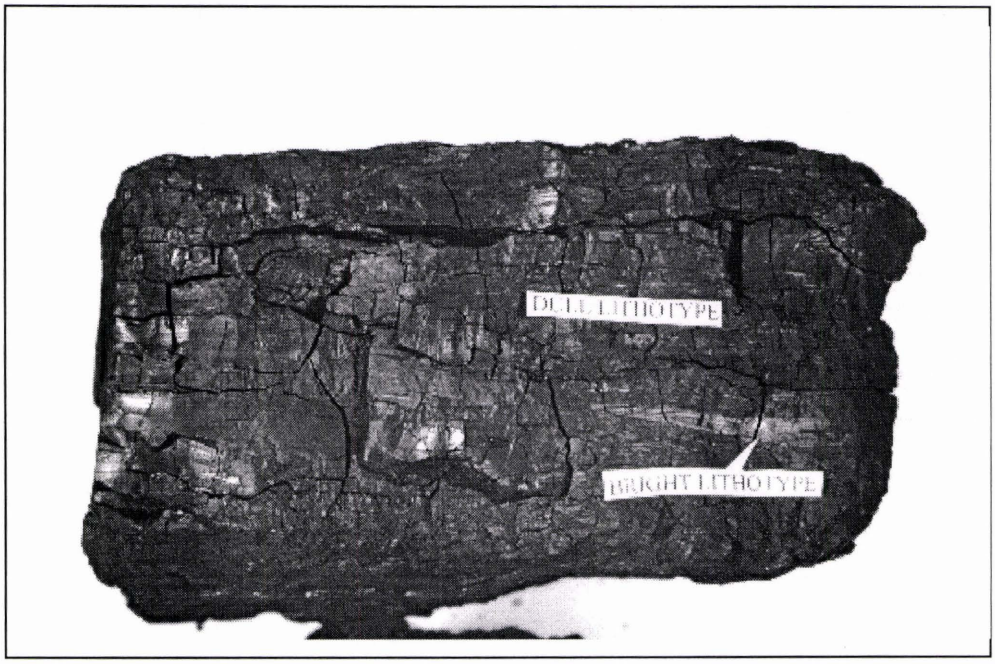

Figure 5. Bright and dull lithotypes in Wyodak subbituminous coal.

beds approximately 6 m thick. The Beulah coal is late Paleocene and is a part of the Sentinel Butte Formation (Groenewold, 1979).

Two lithotypes were prepared from the lignite, 1 kg bright and dull coal. The bright coal occurs as layers 0.5 - 1.5 cm thick. They are hard, smooth, black, and shiny. They are characterized as vitrain. The dull coal does not occur as layers, but acts as a matrix for small included layers of vitrain. The dull appears black, softer than the vitrain, and grainy with a rough texture. Fusain layers are often thick, and incorporate a portion of the dull lithotype. The included layers of vitrain appear to be lenses 1.0-3.0 cm long and 0.0-0.5 cm thick. Maceral, prox/ult, EDXRF, and AEM analyses were performed on the separated lignite lithotypes. Char was not produced from the bright and dull lithotypes due to monetary and time limits. Tables 6-8 provide results obtained from the chemical analyses performed on all of the lithotypes.

Proximate and Ultimate Analyses

The succeeding discussion summarizes the procedures used in proximate and ultimate analyses. The purpose of this discussion is to explain the practical aspects of the two analytical tests briefly and clearly.

Proximate and ultimate analyses were performed on all of the lithotype samples at the UND-EERC. Proximate analysis determines the content of volatile matter, moisture, fixed carbon, and ash expressed in percent by weight. Ultimate analysis provides the percent by weight content of total carbon,

Table 6. Prox/Ult, EDXRF, and maceral analyses for Pittsburgh #8 bituminous lithotyes.

	Pitt. # 8	Bright	Bright w/ Pyrite	Super Bright	Dull
Proximate Analysis, as-received, wt%					
Moisture	2.2	1.70	1.50	1.40	1.40
Volatile Matter	37.8	38.47	36.21	38.54	41.86
Fixed Carbon	52.6	56.50	53.92	58.02	53.00
Ash	7.4	3.33	8.37	2.04	3.74
Ultimate Analysis, as-received, wt%					
Carbon	76.16	80.76	76.07	82.31	81.87
Hydrogen	5.40	5.69	5.30	5.83	5.99
Nitrogen	1.35	1.44	1.48	1.51	1.38
Sulfur	1.58	0.74	1.61	0.88	0.67
Oxygen	8.14	8.04	7.17	7.43	6.35
Ash Composition, % as oxides					
Calcium, CaO	3.3	1.4	1.7	NA	1.8
Magnesium, MgO	0.9	1.6	0.9		1.1
Sodium, Na_2O	0.2	1.3	1.7		2.0
Silica, SiO_2	52.4	55.8	56.2		67.7
Aluminum, Al_2O_3	24.3	33.8	27.6		24.3
Ferric, Fe_2O_3	13.7	7.5	14.8		3.9
Titanium, TiO_2	1.0	1.4	0.8		2.4
Phosphorus, P_2O_5	0.5	0.1	1.5		0.0
Potassium, K_2O	1.6	1.3	1.5		2.3
Sulfur, SO_3	1.9	1.7	1.0		
Heating Value					
moisture-free, MJ/kg	31.0	33.5	31.4	34.0	34.1
as-received, MJ/kg	31.7	32.9	30.9	33.5	33.6

Table 6 cont.

Maceral Analysis, mineral free, vol%					
Vitrinite	83.4	83.0	91.3	85.0	35.5
Liptinite					
Sporinite	3.9	4.1	1.0	2.6	23.1
Resinite	0.2	0.1	0.2	0.0	0.5
Alginite	0.0	0.0	0.0	0.0	0.1
Liptodetrinite	0.0	0.0	0.0	0.0	0.5
Cutinite	0.0	0.0	0.0	0.0	0.0
Inertinite					
Reactive Semifusinite	2.5	2.2	1.6	2.1	5.8
Inert Semifusinite	5.1	4.4	3.1	4.2	11.7
Fusinte	2.1	2.8	1.2	2.2	5.3
Macrinite	0.1	0.0	0.2	0.1	0.4
Micrinite	2.0	2.7	1.4	2.8	14.9
Inertodetrinite	0.9	0.7	0.0	1.0	2.2
Sclerotinite	0.0	0.0	0.0	0.0	0.0
Total Inert Components	10.2	10.6	5.9	10.3	34.5
Total Reactive Components	89.8	89.4	94.1	89.7	65.5

NA = Not Available
Btu/lb = 0.002329 MJ/kg

Table 7. Prox/Ult, EDXRF, and maceral analyses for Wyodak subbituminous lithotypes.

	Bright	Mixed	Dull
Proximate Analysis, as-received, wt%			
Moisture	23.50	22.80	17.60
Volatile Matter	37.66	38.93	45.02
Fixed Carbon	34.01	34.24	27.09
Ash	4.83	4.03	10.29
Ultimate Analysis, as-received, wt%			
Carbon	52.28	53.54	53.71
Hydrogen	6.57	6.49	6.70
Nitrogen	0.66	0.75	0.74
Sulfur	0.84	0.42	0.69
Oxygen	34.82	34.77	10.29
Ash Composition, % as oxides, on an ash basis			
Calcium, CaO	21.5	27.0	15.9
Magnesium, MgO	7.7	10.5	6.3
Sodium, Na_2O	2.0	1.6	1.0
Silica, SiO_2	21.6	22.9	43.6
Aluminum, Al_2O_3	11.6	13.2	9.9
Ferric, Fe_2O_3	7.0	4.7	4.2
Titanium, TiO_2	0.9	1.0	2.3
Phosphorus, P_2O_5	0.4	1.0	0.2
Potassium, K_2O	0.2	0.2	0.2
Sulfur, SO_3	26.9	19.2	15.2
Heating Value, calculated*			
moisture-free, MJ/kg	NA	NA	NA
as-received, MJ/kg	21.6	22.0	23.2
Maceral Analysis, mineral matter free, vol%			
Vitrinite (huminite)	95.6[a]	84.0[b]	81.7[c]
Liptinite			
Sporinite	0.9	1.0	2.9
Resinite	0.3	0.3	0.9
Alginite	0.0	0.0	0.0
Liptodetrinite	0.4	0.8	2.4
Cutinite	0.0	0.2	0.6
Inertinite			
Semifusinite	1.7	10.3	7.7
Fusinte	0.1	1.4	0.6
Macrinite	0.0	0.0	0.0
Micrinite	0.5	0.6	1.4

Table 7 cont.

Inertodetrinite	0.4	1.2	1.2
Sclerotinite	0.1	0.2	0.6
Total Inert Components	2.8	13.7	11.5
Total Reactive Components	97.2	86.3	88.5

*calculated calorific value determined by ASTM method D 3588
[a] mostly ulminite
[b] mixture of attrinite and ulminite
[c] mostly attrinite
NA = Not Available
Btu/lb = 0.002329 MJ/kg

Table 8. Prox/Ult, EDXRF, and maceral analyses for Beulah-Zap lignitic lithotypes.

	Bright	Dull
Proximate Analysis, as-received, wt%		
Moisture	24.90	25.50
Volatile Matter	37.00	35.39
Fixed Carbon	34.21	29.72
Ash	3.90	9.39
Ultimate Analysis, as-received, wt%		
Carbon	49.45	46.37
Hydrogen	6.49	6.25
Nitrogen	0.69	0.68
Sulfur	0.35	0.30
Oxygen	39.11	37.01
Ash Composition, % as oxides		
Calcium, CaO	30.0	17.7
Magnesium, MgO	11.3	9.3
Sodium, Na_2O	5.7	3.6
Silica, SiO_2	18.4	52.9
Aluminum, Al_2O_3	10.8	8.3
Ferric, Fe_2O_3	3.1	2.3
Titanium, TiO_2	0.9	1.6
Phosphorus, P_2O_5	0.3	0.1
Potassium, K_2O	0.3	0.2
Sulfur, SO_3	17.4	7.8
Heating Value, calculated		
moisture-free, MJ/kg	26.3	24.0
as-received, MJ/kg	19.7	17.9
Maceral Analysis, mineral matter free, vol%		
Vitrinite (huminite)	96.2[a]	72.4[b]
Liptinite		
Sporinite	0.3	0.8
Resinite	0.0	0.5
Alginite	0.0	0.0
Liptodetrinite	0.0	0.0
Cutinite	0.3	0.6
Inertinite		
Semifusinite	1.5	19.8
Fusinte	0.2	2.4
Macrinite	0.0	0.2
Micrinite	1.4	1.9

Table 8 cont.

Inertodetrinite	0.0	1.3
Sclerotinite	0.1	0.1
Total Inert Components	3.2	25.7
Total Reactive Components	96.8	74.3

[a] mostly ulminite
[b] mostly attrinite
NA = Not Available
Btu/lb = 0.002329 MJ/kg

hydrogen, sulfur, nitrogen, oxygen, and ash. The two chemical analyses are standard practices prescribing to American Society for Testing Materials (ASTM) standards in common use by the coal and coke industry (ASTM, 1995).

Data provided for the proximate and ultimate analyses for each lithotype sample are reported in four ways: as-determined, as-received, moist-free, and moist- and ash-free. The properties of interest obtained with the as-determined basis are provided after conditioning and preparation of the coal sample to 250-μm sieve in accordance with ASTM Method D 2013 (ASTM, 1995). The as-determined values represent data determined at the time of analysis. The as-received basis reports calculated values with the assumption that the sample arrived at the lab with no loss or gain in moisture. The moist free basis reports the data calculated on a theoretical base of no moisture associated with the sample (ASTM, 1995). The moist- and ash-free basis provides data with the assumption that the sample contains no moisture or ash (ASTM, 1995). The difference between the as-determined and as-received bases is: moisture is determined before processing of the sample in the as-received basis, and moisture content is obtained after processing in the as-determined basis. The lithotype samples in this study were exposed to a warm and dry laboratory atmosphere for many days during the separation process. Therefore, it is assumed that moisture contents were depleted to an unknown degree.

Proximate Analysis

Moisture content is determined by air-drying the coal sample in an oven at 110 degrees Celsius until the weight remains constant. The weight percent loss is the moisture content. Volatile matter is the fraction of coal that is liberated as gas or vapor when heated to 950 degrees Celsius and maintained for seven minutes (ASTM, 1995). The loss in weight minus the moisture content is the volatile matter content. Ash represents the noncombustible components remaining after total combustion of the coal. The physical and chemical properties of the ash is a function of the inorganic components in the original coal, although it has a different size and composition distribution as compared to the original mineral components. One gram of the coal sample is pulverized to 250μm and placed in an oven. The temperature is raised to 700 to 750 degrees Celsius over a period of two hours. The temperature is held at this point for an additional two hours. The ash content is the weight of the residue remaining after the four hour test period. Fixed carbon is the solid combustible matter remaining after pyrolysis that determines the rank of coal having 69% or more fixed carbon (high rank coal) on the dry, mineral-matter-free basis. The fixed carbon content is found by subtracting the sum of moisture, volatile matter, and ash weight percents from 100. Rank for coals having less than 69% fixed carbon is determined by gross calorific values (btu/lb) on a moist, but mineral-matter-free basis.

Ultimate Analysis

Standard practice for chemically analyzing coal is to perform the proximate and ultimate analyses together. The total carbon and hydrogen in a coal sample are determined in a single test. The total carbon represents carbon in the form of volatile matter, fixed carbon, and of carbonates (ASTM, 1995). The hydrogen content represents all the hydrogen in the sample. A weighed quantity of sample is burned and the products of combustion are fixed in an absorption train after complete oxidation and purification. Total carbon and hydrogen percentages are then determined as analyzed (ASTM, 1995). Sulfur content is analyzed using the Eschka Method. A weighed coal sample is combined with Eschka mixture, and ignited. Barium sulfate is precipitated from the solution mixed in hot water. The sulfur weight percent is then determined by ASTM methods. Nitrogen concentration is measured by converting all nitrogen to ammonia as described in the Annual Book of ASTM Standards, section 5, 1995. Ammonia is recovered by a distillation process and measured by titration analysis (ASTM, 1995). The oxygen weight percent is calculated from summing the percent by weight carbon, hydrogen, sulfur, and ash, and subtracting from 100.

Results

Pittsburgh #8 Bituminous Lithotypes

Samples submitted for proximate and ultimate (prox/ult) analyses from the Pittsburgh #8 coal seam include: Pittsburgh #8 (mother coal from which the others were separated), bright, super bright, bright with pyrite, and dull. Figure 6 shows the results of the prox/ult tests for the bituminous samples. By ASTM standards each lithotype sample can be classified as High-Volatile A Bituminous Coal. The only significant difference occurs in ash content between the bright with pyrite and the other three samples. The dull, bright, and super bright samples have weight percentages for ash ranging from 2 to 3% on an as-received basis. The bright with pyrite sample has 8% ash on an as-received basis.

Wyodak Subbituminous Lithotypes

The bright, dull and mixed lithotype samples have nearly identical calculated calorific values comparable to subbituminous coal, according to ASTM protocol. The heating values were not determined in the lab and, therefore it is assumed that all of the lithotype samples are of subbituminous rank. The dull sample has the most ash and the least amount of moisture, volatile matter, and fixed carbon associated with it. The bright and mixed samples have nearly identical prox/ult results. It is partly evident from the analysis that the dull sample

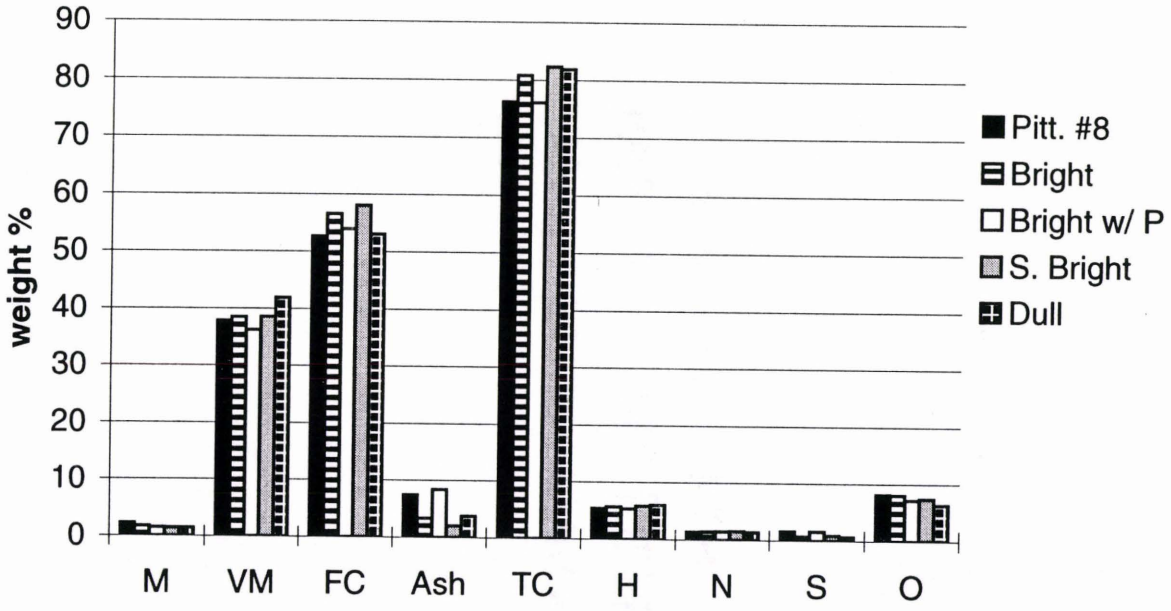

Proximate analysis parameters

M= moisture
VM= volatile matter
FC= fixed carbon
ash= inorganic components

Ultimate analysis parameters

TC= total carbon
H= hydrogen
N= nitrogen
S= sulfur
O= oxygen

Figure 6. Proximate and ultimate analyses for Pittsburgh #8 bituminous lithotypes on as-received bases.

is chemically and physically different from the other two lithotype samples. Refer to Figure 7 for prox/ult results.

Beulah-Zap Lignitic Lithotypes

Both the bright and dull samples of the Freedom lignite have heating values on an as-received basis of approximately 8000 btu/lb. This value corresponds to lignite A coal as defined by ASTM. The dull and bright samples have 9% and 4% ash, respectively, on an as-received basis. Results from the remaining components of the prox/ult test for the two samples are in accordance to each other (Figure 8).

Maceral Analyses

Maceral analyses show important information regarding chemical compositions and origins of the different lithotypes separated from the bituminous, subbituminous, and lignitic coals. Bright lithotypes were separated in order to obtain high percentages of vitrinite and liptinite macerals. Dull lithotypes were collected to obtain high amounts of inertinite. The maceral analyses show that separation of the different parts of the coal provide lithotype samples enriched either in vitrinite or inertinite macerals. Figures 9, 10 and 11 show the abundance of the major macerals for lithotypes separated from bituminous, subbituminous, and lignitic coals.

The Coal and Organic Petrology Laboratories, Pennsylvania State University performed the maceral analyses. Preparation and analysis of the

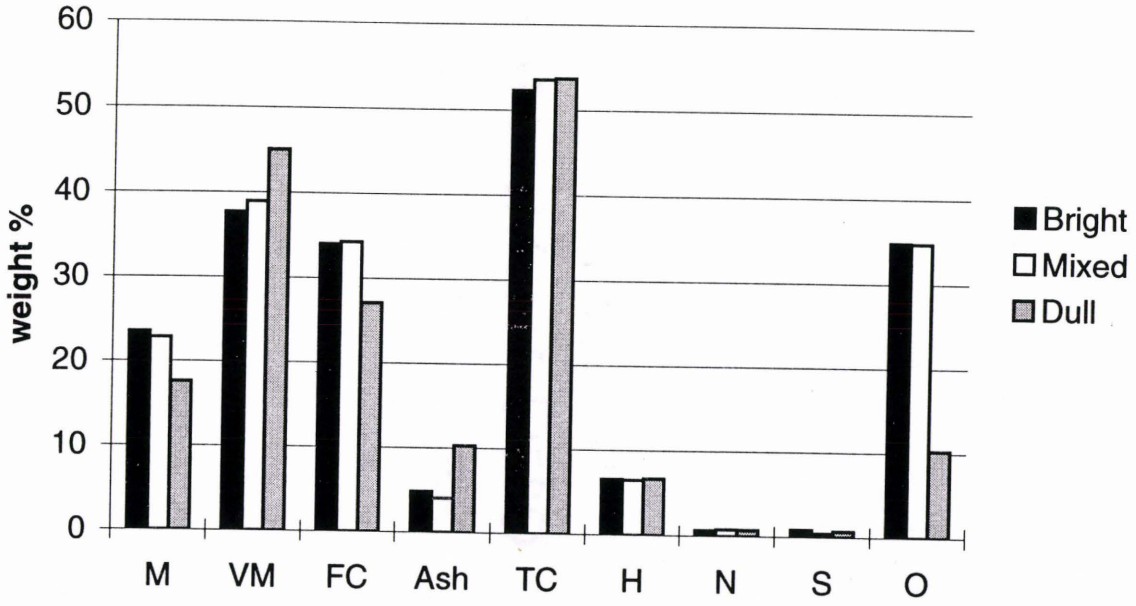

Proximate analysis parameters

M= moisture
VM= volatile matter
FC= fixed carbon
Ash= inorganic components

Ultimate analysis parameters

TC= total carbon
H= hydrogen
N= nitrogen
S= sulfur
O= oxygen

Figure 7. Proximate and ultimate analyses for Wyodak subbituminous lithotypes on as-received bases.

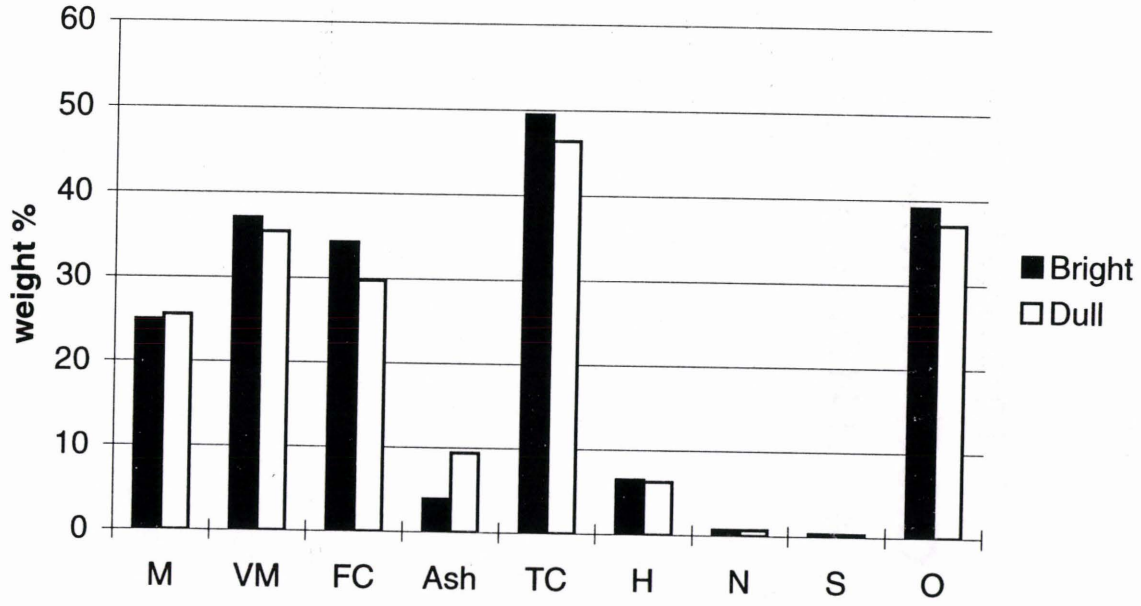

Proximate analysis parameters

M= moisture
VM= volatile matter
FC= fixed carbon
Ash= inorganic components

Ultimate analysis parameters

TC= total carbon
H= hydrogen
N= nitrogen
S= sulfur
O= oxygen

Figure 8. Proximate and ultimate analyses for Beulah-Zap lignitic lithotypes on as-received bases.

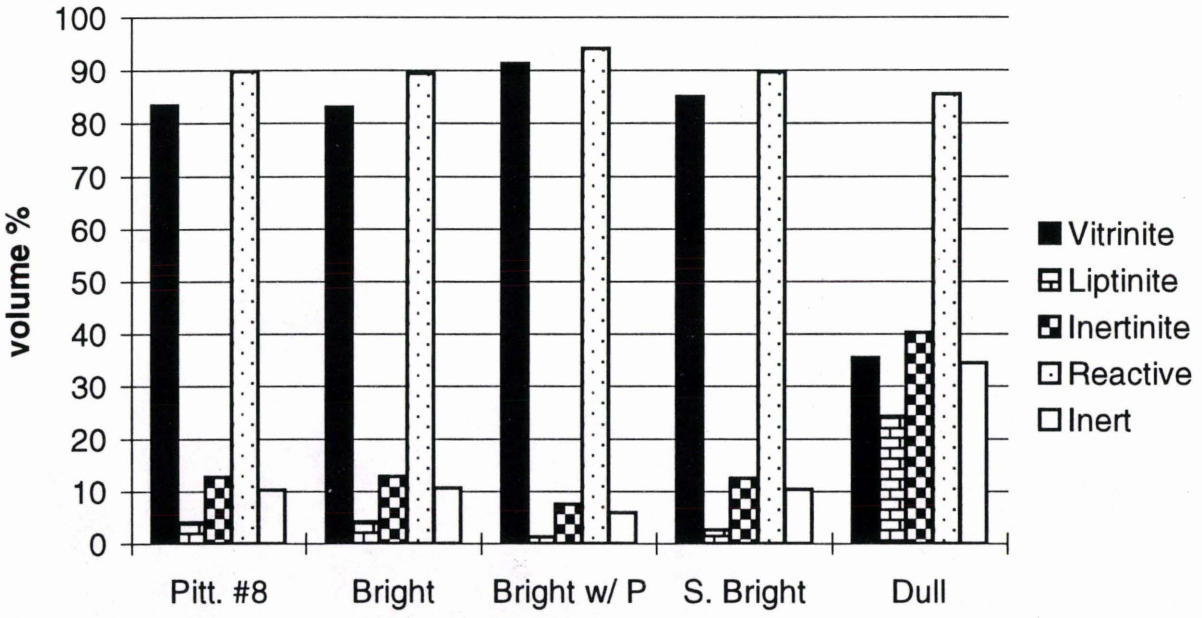

Figure 9. Maceral content of Pittsburgh #8 bituminous lithotypes.

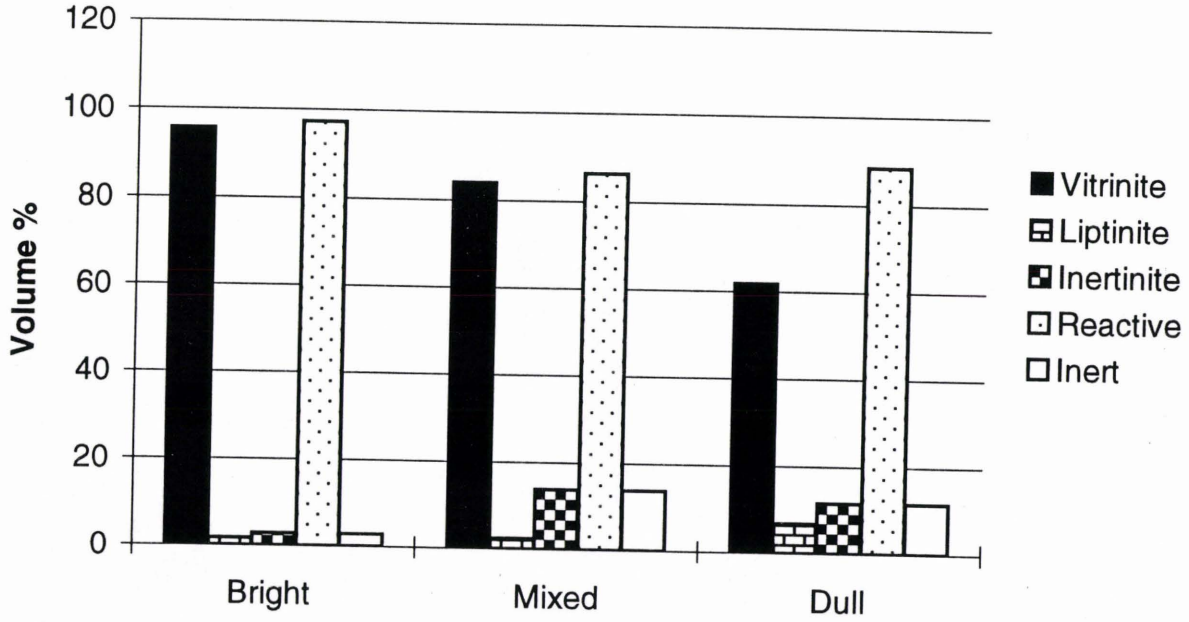

Figure 10. Maceral content of Wyodak subbituminous lithotypes.

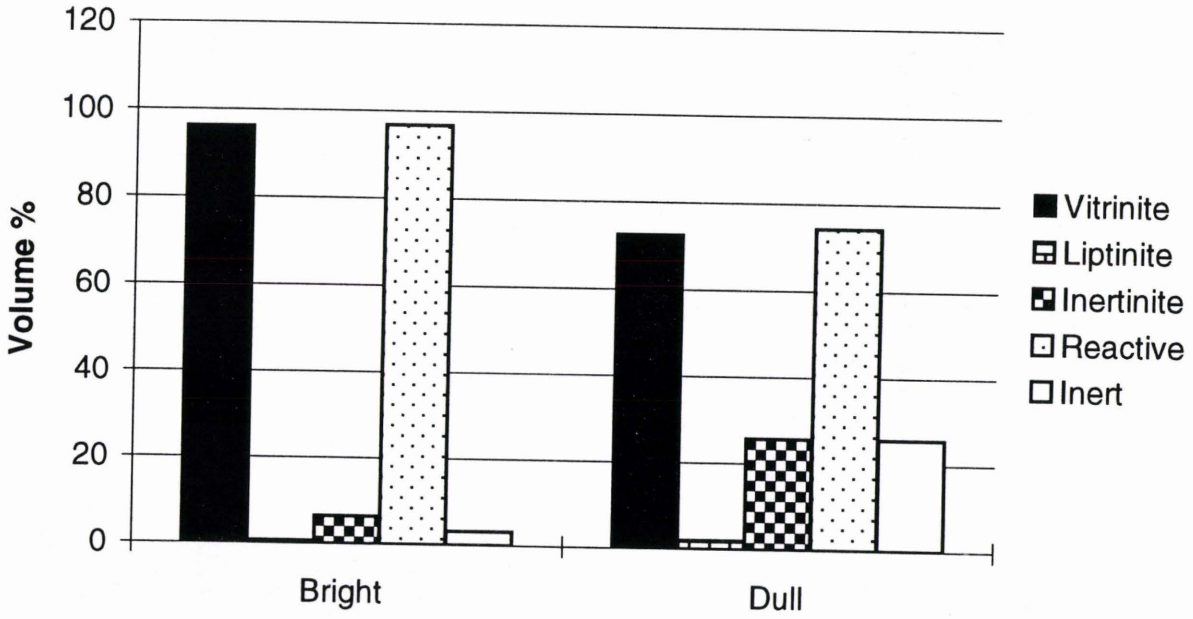

Figure 11. Maceral content of Beulah-Zap lignitic lithotypes.

lithotypes followed ASTM D2797 protocol. The analyses are reported on a mineral-matter-free basis. Refer to Gerencher (1983) for specific procedures for maceral analysis used by Pennsylvania State University.

Five samples collected from the bituminous coal were submitted for maceral analyses: Pittsburgh #8, dull, bright with pyrite, bright, and super bright. The Pittsburgh #8 sample is the parent coal from which the other samples were separated. This sample contains mostly vitrinite macerals, 83%. Liptinite macerals constitute 6% of the sample, and inertinite makes up 10%. The dull lithotype is typical durain, consisting of 36% vitrinite, 24% liptinite (mostly sporinite), and 40% inertinite macerals. The macerals are intimately mixed and packed tightly within each lithotype particle forming a dense blocky coal. The bright with pyrite lithotype sample contains 91% vitrinite, 1% liptinite, and 8% inertinite macerals. The pyrite in this sample occurs as 10-20 micron size blebs and clusters of crystals 1-5 microns. The bright sample consists of 83% vitrinite, 4% liptinite, and 13% inertinite macerals. Eighty five percent vitrinite, 3% liptinite, and 12% inertinite macerals comprise the organic fraction of the super bright lithotype. Sporinite is the most abundant liptinite maceral, and semifusinite, fusinite and micrinite are the major inertinite macerals present in all of the bituminous lithotype samples.

The three lithotype samples separated from the subbituminous coal and submitted for maceral analyses are bright, mixed, and dull. Maceral content for

the subbituminous lithotypes can be described using brown coal terminology according to the ICCP, because the preservation-state of the organic material is noticeable. The dull lithotype contains the least amount of huminite macerals whereas the bright lithotype has the most. Liptinite macerals are not very abundant in any of the lithotypes, but are more common in the dull lithotype. Attrinite is the principal maceral making up the huminite macerals in the dull lithotype. Inertinite and liptinite macerals are disseminated evenly within the fine matrix of attrinite. Ulminite is the huminite maceral constituting most of the bright lithotype. The mixed lithotype contains nearly equal proportions of ulminite and attrinite macerals. Inertinite and liptinite macerals are associated with the mixed lithotype differently than in the bright and dull lithotypes. The attrinite portion of the mixed lithotype is not as granular as in the dull lithotype and the inertinite is present in larger size fragments. Therefore, it can be concluded that the mixed lithotype is not purely a mixture of bright and dull layers, but is a separate lithotype. Further analysis is needed to explain these differences.

Bright and dull lithotypes collected from the lignitic coal were submitted for maceral analyses. Because plant tissues are recognizable, the brown coal terminology for the different lithotypes is used. The bright lithotype contains much more huminite and less inertinite macerals than the dull lithotype. Ulminite, particularly corpohuminite, is the major maceral found in the bright lithotype. The dull lithotype is composed of mostly ulminite associated with some

attrinite. Very little liptinite macerals occurs in either lithotype. The inertinite and liptinite macerals are present as fine-sized particles or in thin layers within the huminite matrix in the bright lithotype. Inertinite, namely semifusinite, occurs as thick lenses or coarse fragments in the huminite matrix of the dull lithotype.

The maceral analyses for the different lithotypes show that megascopic differences correspond during microscopic examination and that in general the dull lithotypes contain more inertinite and the bright lithotypes contain more vitrinite. Consequently, the dull lithotypes are referred to as inert and the bright lithotypes, reactive.

Energy Dispersive X-ray Fluorescence

Energy dispersive X-ray fluorescence spectroscopy (EDXRF) was used at the UND-EERC to determine elemental composition for the ash produced by the different lithotypes. The lithotype samples are ashed, crushed into a fine powder, and, then compressed into a pellet. As X-rays irradiate the specimen, electrons are dislodged from the innermost shells, and electrons from the next highest energy level replace the dislodged electrons. The cascading of electrons from higher to lower energy shells emit energy in the form of characteristic X-radiation (Klein and Hurlbut, 1993). A spectrometric detector determines these characteristic secondary X-rays.

The ash is tested for Si, Al, Fe, Ti, P, Ca, Mg, Na, K, and S. They are presented in oxide concentrations normalized to a closure of 100%. EDXRF

data is represented in Figures 12,13 and 14. Bright, dull, and bright with pyrite lithotype samples for the bituminous coal were submitted for EDXRF analyses. The bright and dull samples produced significant amounts of silicon- and aluminum-rich ash. Ash associated with the bright with pyrite lithotype contained more iron than the ash associated with the bright and dull lithotypes. Calcium, magnesium, and sulfur are more abundant in all of the lithotypes separated from the subbituminous coal than in the bituminous lithotypes analyzed. Silicon and aluminum are principal elements present in ash of the three subbituminous lithotypes. There are no major differences regarding elemental compositions of ash between the different lithotypes in the subbituminous coal. The bright and dull lithotypes separated from the lignitic coal differ significantly in regards to the EDXRF analyses. The ash of the bright lithotype contains more calcium, magnesium, and sulfur, and less silicon than that of the dull.

A major difference between bright and dull lithotypes in all of the coals is silicon appears to most abundant in ash produced by the dull lithotypes, whereas calcium, magnesium, and sulfur are more abundant in the ash from the bright lithotypes. This difference may be related to the mode of deposition for the different lithotypes. The dull lithotypes may have been deposited in deeper water where detrital, silicon-rich sediment accumulated. The bright lithotypes may have been deposited in shallower water where deposition of detrital

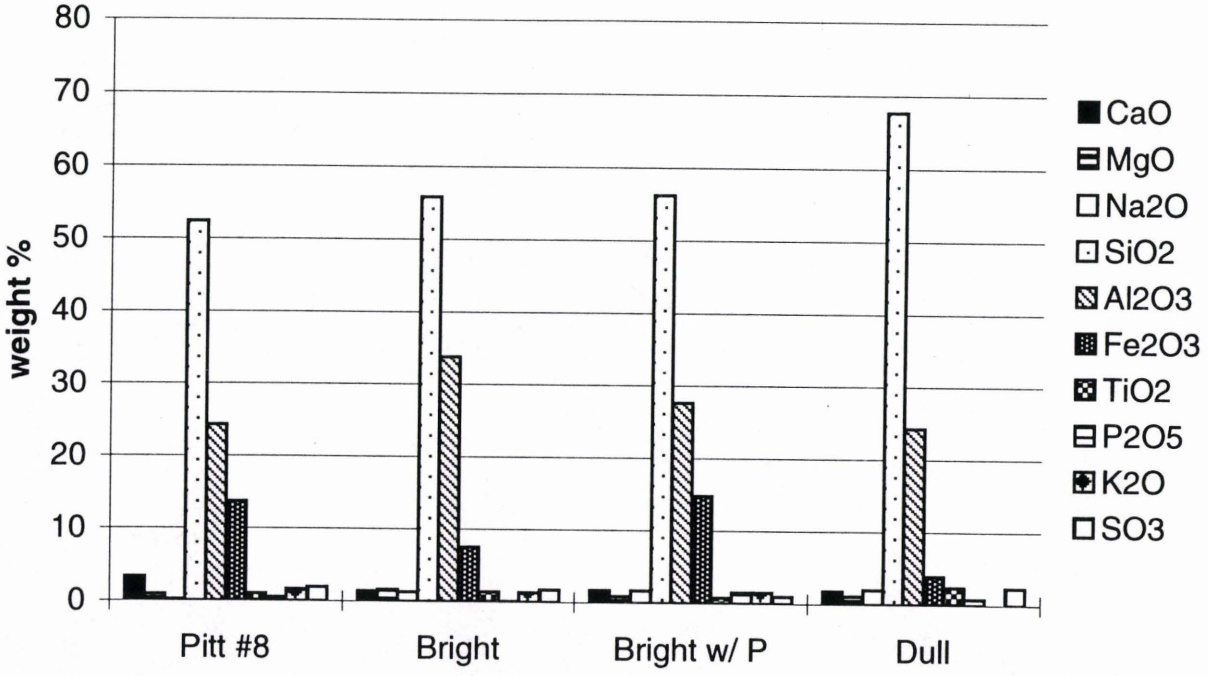

Figure 12. Ash compositions for Pittsburgh #8 bituminous lithotypes on an oxide basis.

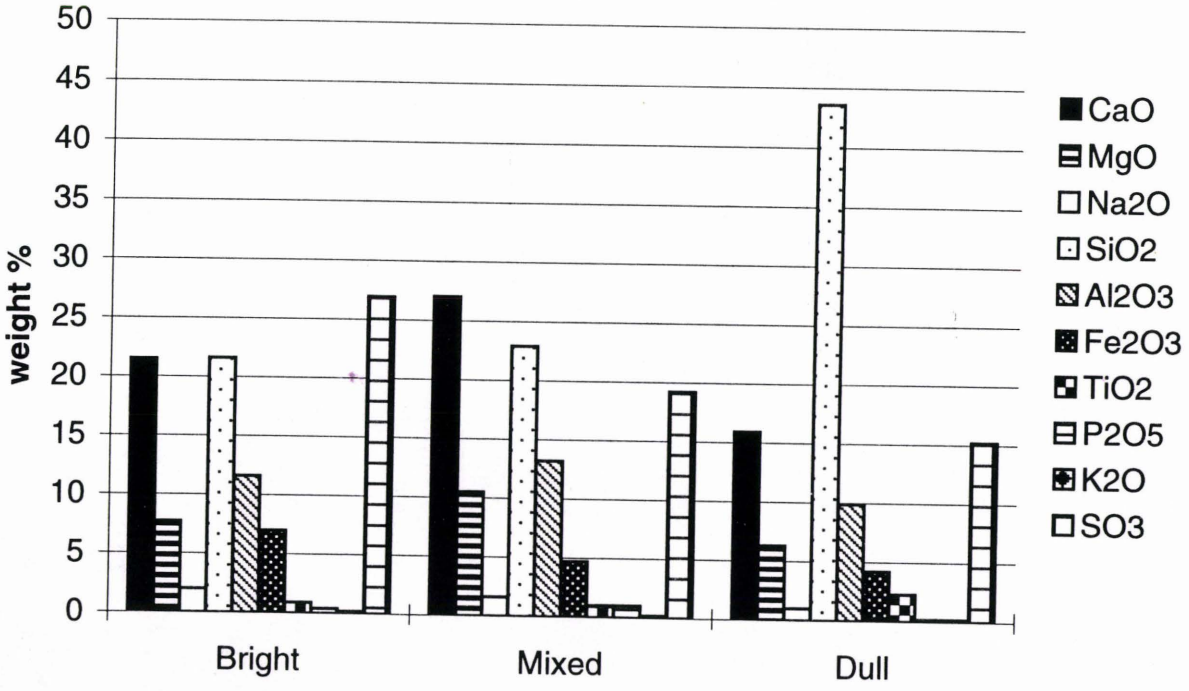

Figure 13. Ash compositions for Wyodak subbituminous lithotypes on an oxide basis.

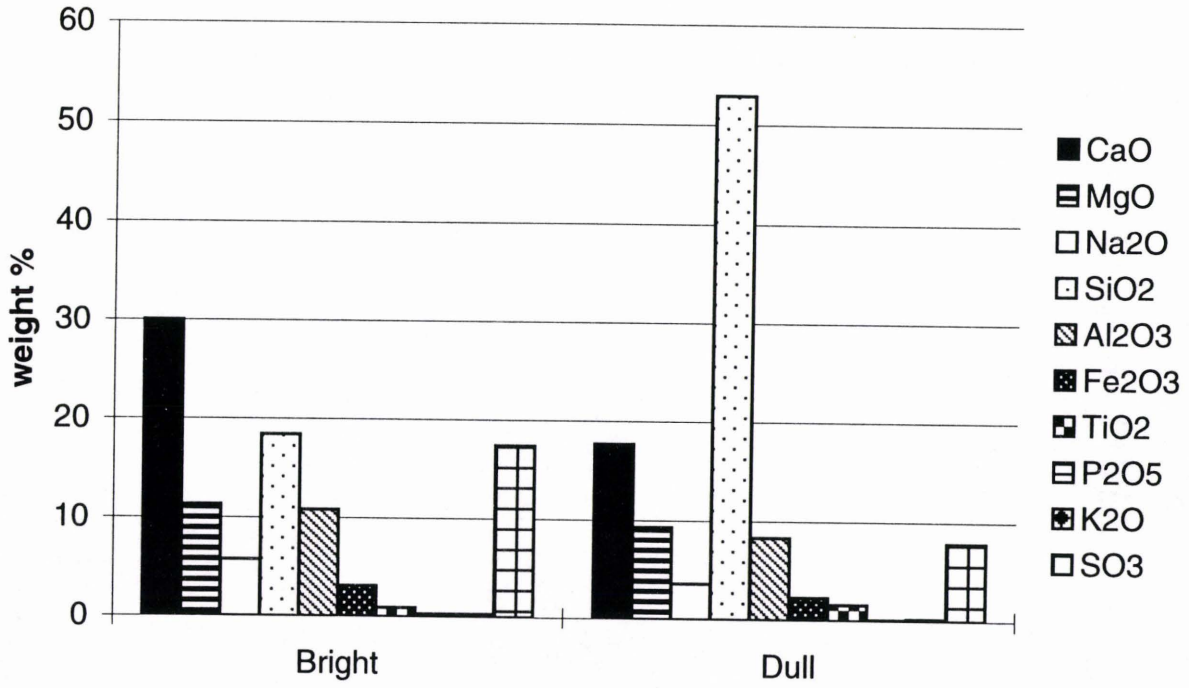

Figure 14. Ash compositions for Beulah-Zap lignitic lithotypes on an oxide basis.

sediment is inhibited. Of course, further examination is necessary to test this hypothesis.

Analytical Electron Microscopy

Analytical electron microscopy (AEM) was used to study the bright and dull lithotypes, and on char produced by bright and dull lithotypes. The HF-2000 Field Emission Gun Analytical Electron Microscope was used at the High Temperature Materials Laboratory (HTML), Oak Ridge National Laboratories (ORNL). The HF-2000 is a 200 KeV transmission electron microscope (TEM) equipped with a field emission gun with a single crystal tungsten emitter. Thin sections of bright and dull lithotypes and char were prepared by an ion beam mill to determine with the TEM if there are certain mineral types and sizes, specifically nanometer-scale inorganic components that are enriched in each sample. The TEM was also used to identify different char morphologies produced from bituminous and subbituminous coals.

Lithotype Analyses

Abundant nanometer-scale inorganic inclusions as had been observed previously (Hurley and Schobert, 1992) were not evident in the bright and dull coal lithotype samples prepared and analyzed at ORNL. Therefore, ultramicrotome thin sections of each coal sample and char were prepared and investigated with a non-analytical TEM at University of North Dakota (UND) and with energy dispersive spectroscopy at ORNL at a later date. Using this

preparation procedure, abundant nanometer-sized particles are apparent in the subbituminous bright lithotype that may lead to the formation of submicron ash (Figure 15 and 16). The spherical inclusions are 2.5-5 nm in diameter and are uniformly disseminated in the lithotype particle. Figure 17 and 18 shows inclusions 7-20 nm in another subbituminous bright lithotype particle.

AEM was used at ORNL in the second session to identify the nanometer-scale inclusions found in the subbituminous lithotype at UND. They were not observed at ORNL. While using the TEM at ORNL, differentiation between epoxy (medium embedding particles), coal particles, and formvar (backing support on sample grid) was extremely difficult. This discrepancy can be related to many factors including differences in electron beam voltage used in the TEM at UND and the TEM at ORNL, 80 KeV and 200 KeV respectively.

Approximately 90 X-ray spectra were obtained from individual mineral inclusions, and from coal matrices using energy dispersive spectroscopy (EDS). EDS is very similar to electron probe microanalysis and X-ray fluorescence analysis. In EDS and electron probe microanalysis, an electron beam focused to very small diameters irradiates the specimen, dislodging inner shell electrons. Higher energy electrons cascade down to fill the lower energy shells, and consequently lose energy in the form of X-rays. A crystal spectrometer detects the characteristic X-rays in electron probe microanalysis, whereas an energy

Figure 15. TEM photograph of an ultramicrotome thin section of a subbituminous bright lithotype particle containing abundant nanometer-scale inclusion.

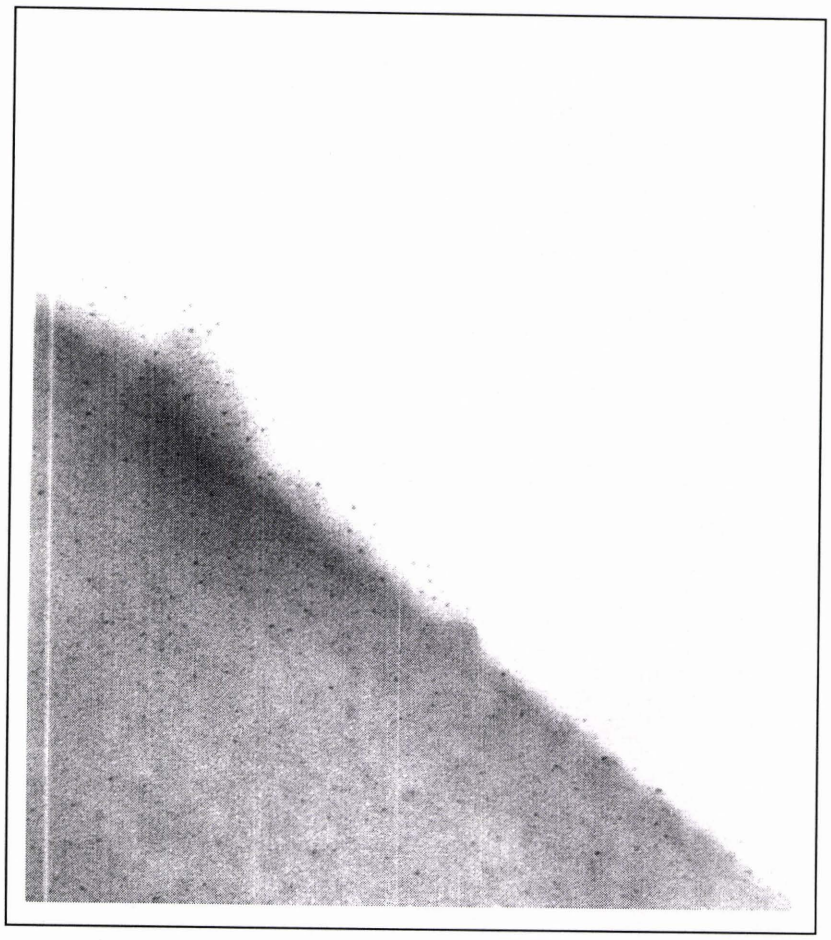

Figure 16. TEM photograph of 2.5-5 nm-diameter inclusions in the subbituminous dull lithotype particle shown in Figure 15.

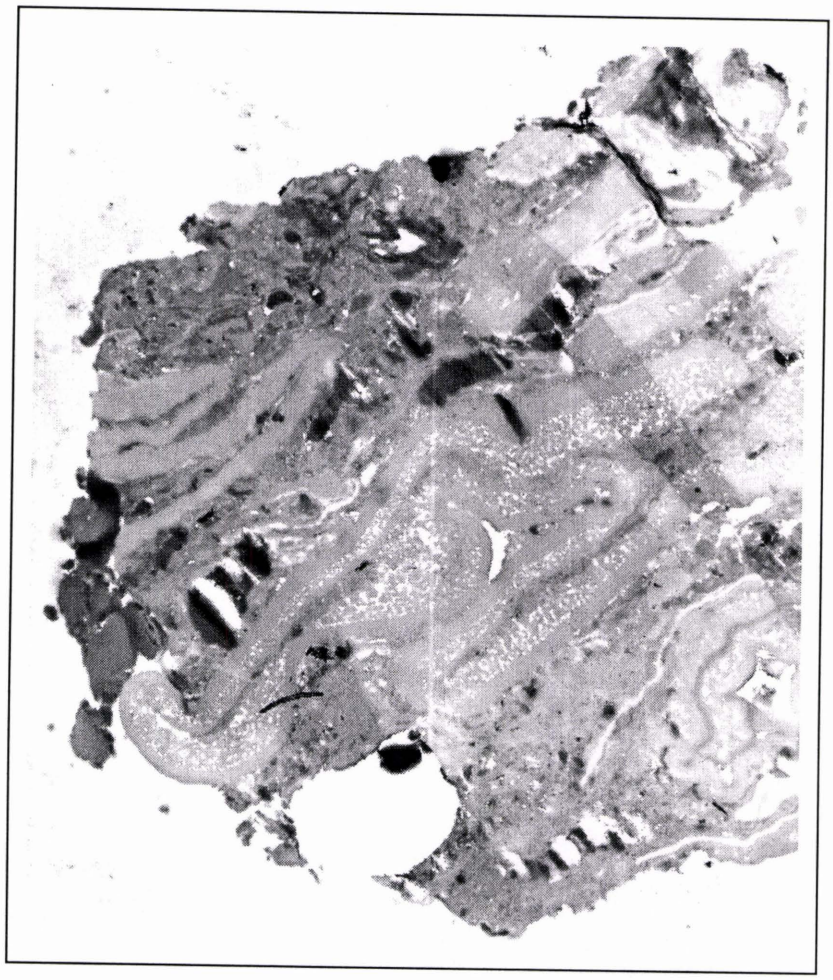

Figure 17. TEM photograph of an ultramicrotome thin section of a subbituminous bright lithotype particle containing abundant nanometer-scale inclusions.

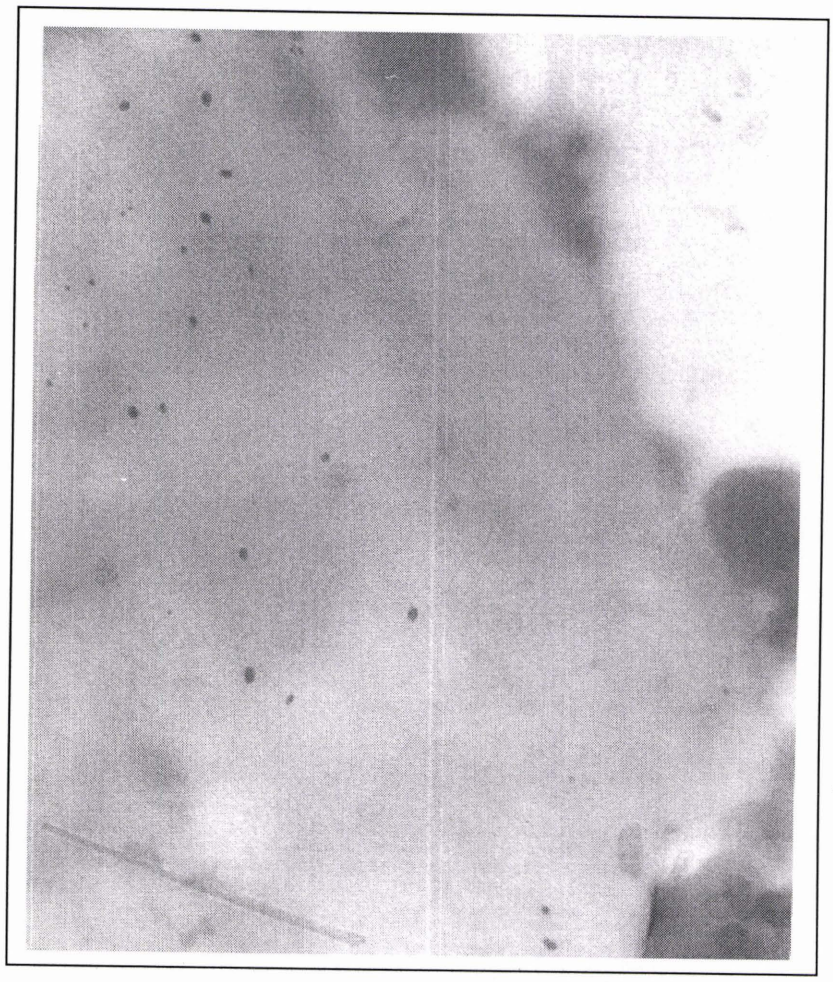

Figure 18. TEM photograph of 7 – 20 nm-diameter inclusions in the lithotypes particle shown in Figure 17.

dispersive X-ray analysis system acts as the detector in EDS (Klein and Hurlbut, 1993). The EDS system at ORNL has a spatial resolution of 1-nm.

EDS performed on the lithotypes indicates that organically-bound inorganic elements prevalent in the subbituminous lithotypes and more so in the lignitic lithotypes may contribute to the stickiness of ash deposits on high temperature filters used in coal-fired power plants. Organically-bound inorganic elements refers to inorganic elements that are usually common in inorganic compounds that are attached to or associated with organic compounds. Figures 19-22 show X-ray spectra obtained by EDS for subbituminous and lignitic lithotypes. To the contrary, the bituminous lithotypes had little organically-bound inorganic elements (Figures 23 and 24). Mineral inclusions ranged in size from several nanometers to several microns, the larger being more abundant. Aluminum oxides, titanium oxides, and aluminum silicates made up the majority of submicron inorganic inclusions analyzed. The EDS analyses performed is qualitative rather than quantitative, in that only presence of certain elements was tested. In order to obtain information on which phases of certain polymorphs are present, standards need to be made or electron diffraction is necessary. Due to time constraints, neither of these analytical techniques was achieved.

Analysis of Inorganic Inclusions in Char

A second objective of this study is to determine the morphology of char that certain lithotypes produce after partial combustion, and to characterize the

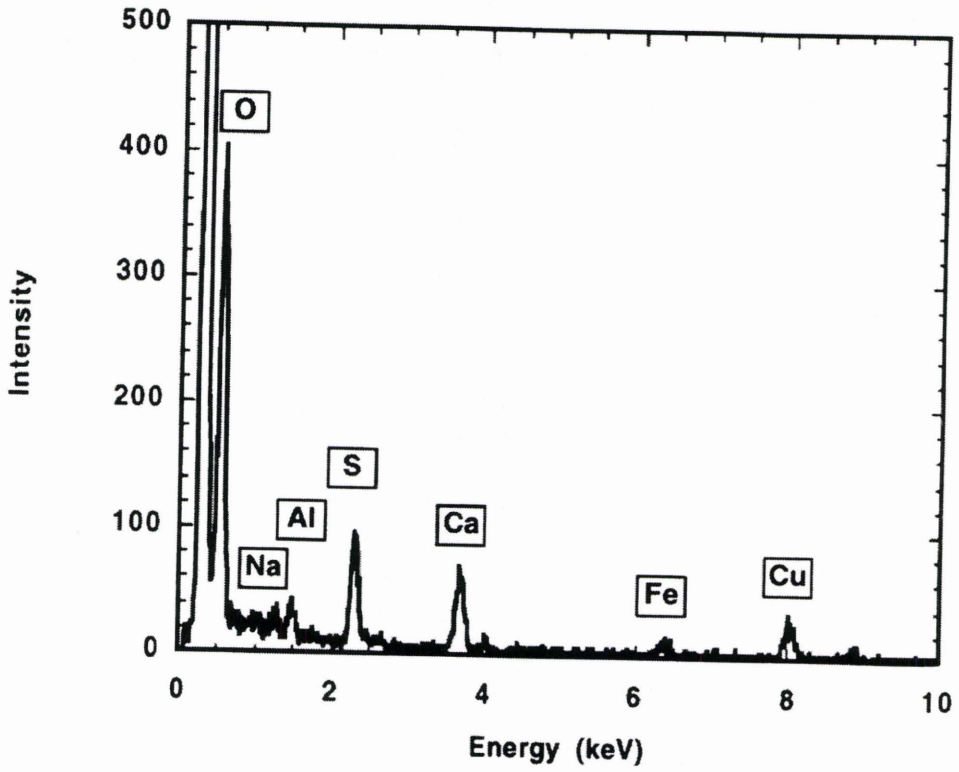

Figure 19. Regular elemental composition for subbituminous bright lithotypes. The Cu peak is a result of the TEM specimen grid.

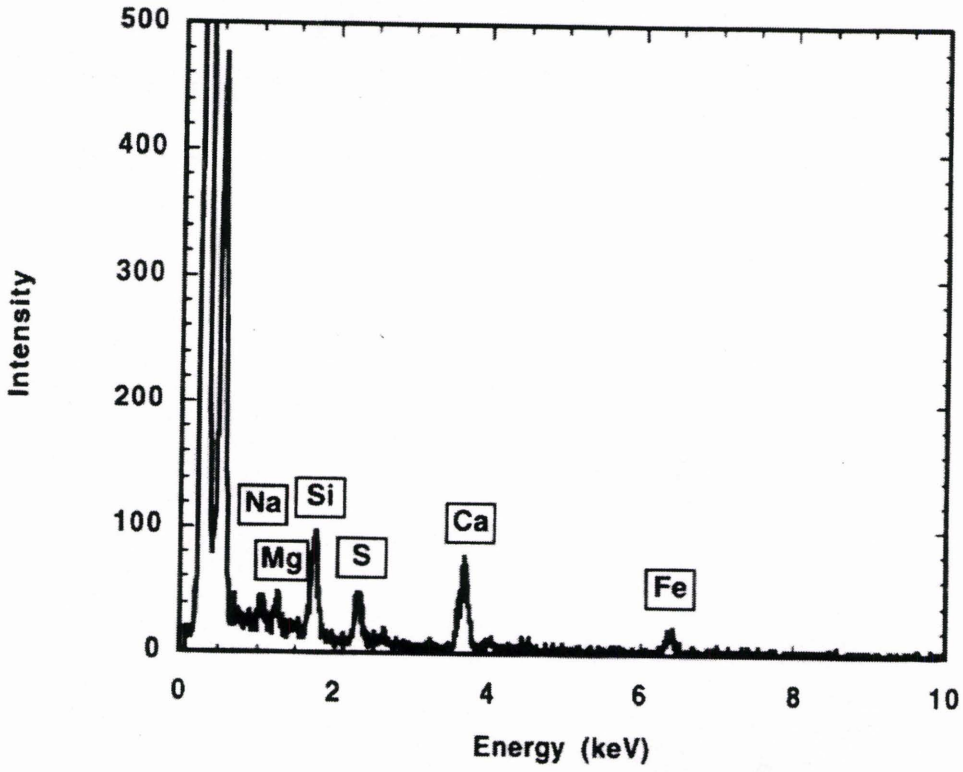

Figure 20. Regular elemental composition for subbituminous dull lithotypes.

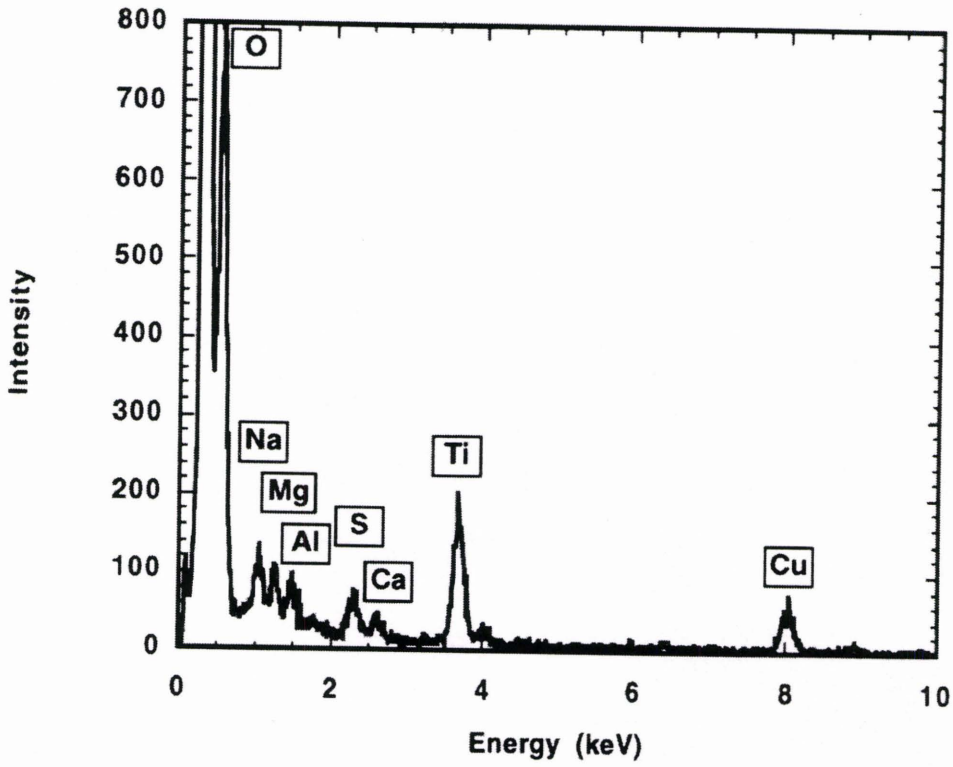

Figure 21. Regular elemental composition for lignitic bright lithotypes. The Cu peak is a result of the TEM specimen grid.

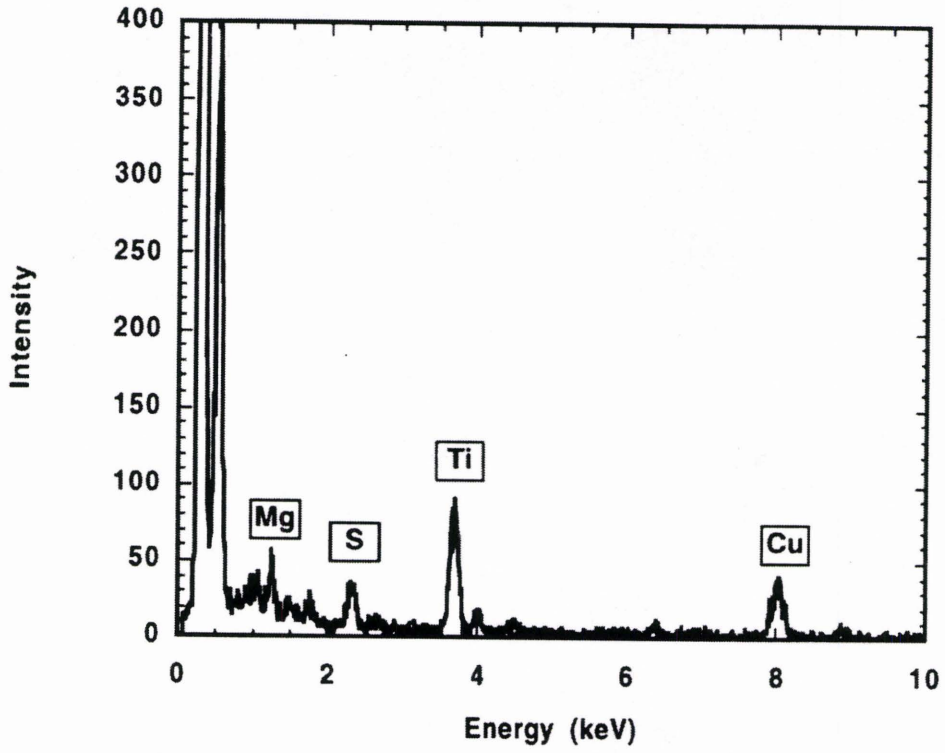

Figure 22. Regular elemental composition for lignitic dull lithotypes. The Cu peak is a result of the TEM specimen grid.

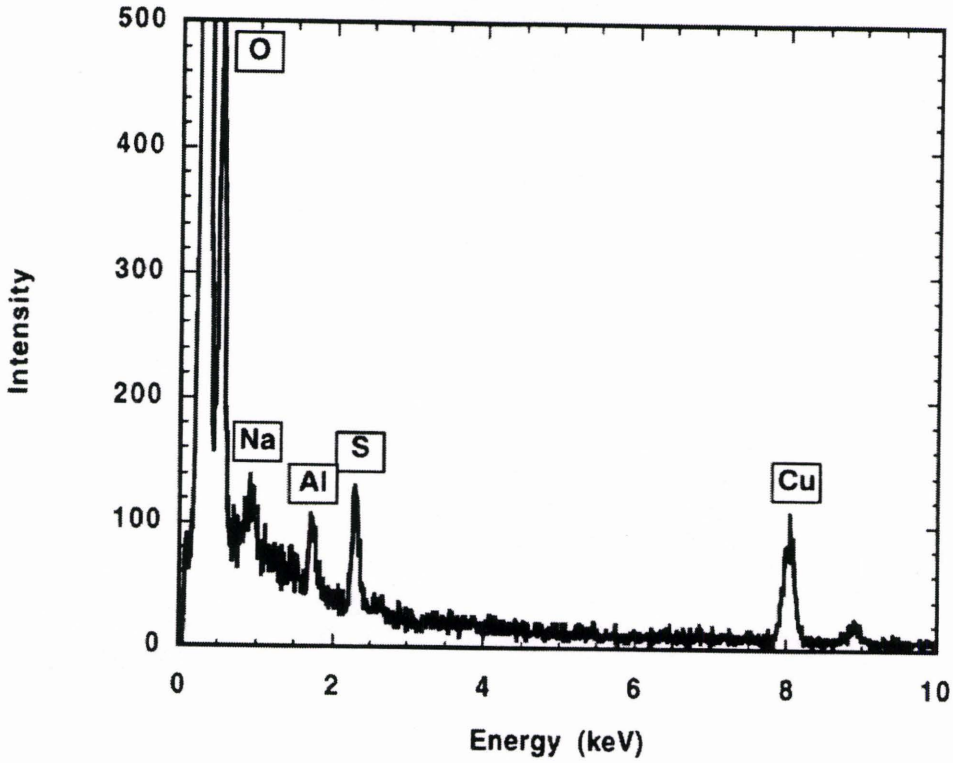

Figure 23. Regular elemental composition for bituminous bright lithotypes. The Cu peak is a result of the TEM specimen grid.

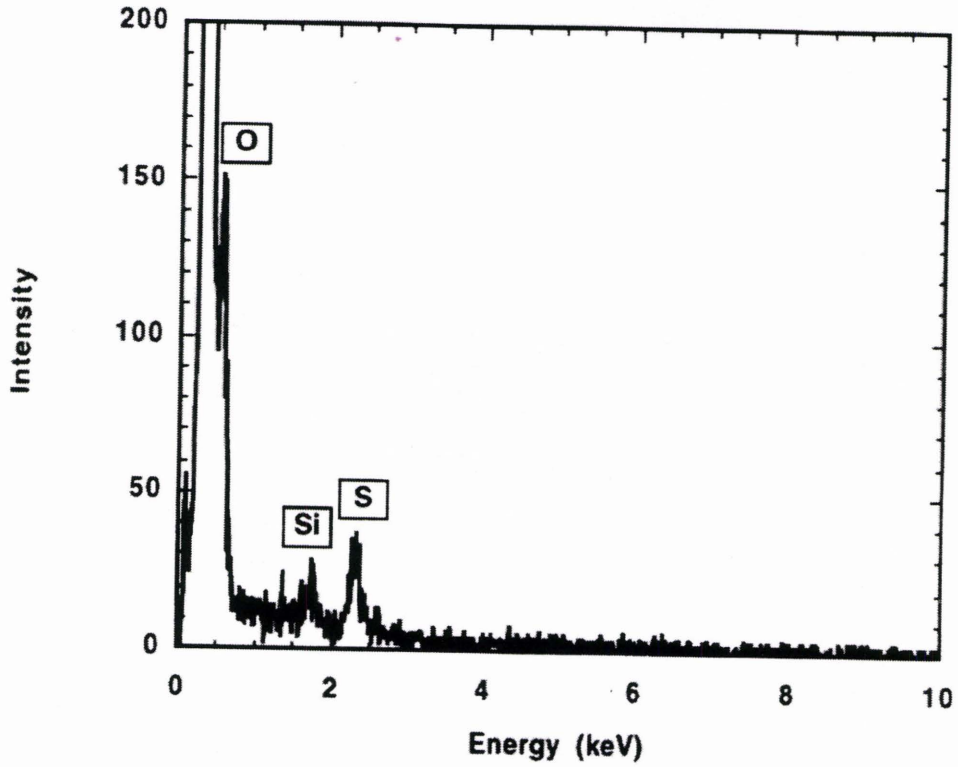

Figure 24. Regular elemental composition for bituminous dull lithotypes.

nanometer-scale components in each char particle. Char and ash were produced by a bench-scale pressurized fluidized-bed combustor (PFBC) at the UND-EERC. The char was collected with an isokinetic probe, and then aerodynamically sized by a multicyclone system. The amount of coarse and fine ash collected by the multicyclone system were very similar, and therefore it is concluded that bright and dull lithotypes do not influence the size of ash in a PFBC, but may have an effect in other types of coal-fired combustion systems.

The ultramicrotome thin sections of char rendered problems similar to difficulties associated with the ultramicrotome thin sections of the lithotypes when viewed with the TEM at ORNL. Consequently, powder samples were prepared. Mortar and pestle were used to crush the char and ash grains that were then sprinkled onto meshed, copper grids. The edges of most char and ash particles were as thin as 40 nm, but morphologies may have been lost due to pulverizing.

Using analytical transmission electron microscopy at ORNL high carbon content in char produced intense carbon peaks on all EDS spectra. The copper grid supporting the char particles produces copper peaks. Inorganic nanometer-scale components were found in all of the powder char samples. They are subhedral and show diffraction characteristics, much like the euhedral particles seen by Hurley and Schobert (1993). They typically occur as groups of 10-30 inclusions that range in size from 5-70 nm in cross section. Calcium peaks are characteristic of EDS spectra obtained from nanometer-scale components in all

of the char particles analyzed. Titanium peaks dominate EDS spectra acquired from analysis of the small particles in the bituminous char. Aluminum appears to be abundant in the nanometer-scale inorganic components in the char produced from the bituminous bright lithotype. Iron is common in the nanometer-scale particles in the subbituminous char. Table 9 summarizes the relative energy dispersive peak intensities produced by char matrices and included nanometer-scale components.

Pittsburgh #8 Bituminous Char

Two size classes of nanometer-scale inorganic components are recognized in the bituminous bright char, 10-20 nm and >30 nm. Energy dispersive peak intensities are strong for titanium and aluminum in all of the components in the 10-20 nm size class. Iron and calcium are present in many of the inclusions of both size classes. Inclusions >30 nm in size contain silicon and calcium. Sulfur is also present in some of the inclusions >30 nm. Carbon and oxygen energy dispersive peak intensities are strong for all char matrices in the char produced by the bituminous bright lithotype. Figure 25 shows a region in a char particle containing inorganic components 10-20 nm in diameter. The lightest area in the figure is epoxy. The darkest area is a thick region of the char particle. Elemental compositions for the char matrix and of nanometer-scale particles are shown in Figures 26 and 27.

Table 9. Relative X-ray intensities shown by EDS for char matrices and included nanometer-scale inorganic particles. Relative energy dispersive intensities are semi-quantitative.

	Relative Energy Dispersive Intensities							
	Char Matrices				Nanometer-Scale Inorganic Inclusions			
	Bituminous		Subbituminous		Bituminous		Subbituminous	
	Bright	Dull	Bright	Dull	Bright	Dull	Bright	Dull
Element								
Carbon	high	high	high	NA	high	high	high	NA
Oxygen	high	high	high		high	high	high	
Magnesium	low	low-medium	medium-high		≈zero	low	medium	
Aluminum	low	low-Medium	medium		high	low	low	
Silicon	low	low-medium	low-medium		≈zero	low	low	
Sulfur	low	low-medium	high		≈zero	low	medium	
Calcium	≈zero	low	high		≈zero	low	medium	
Titanium	≈zero	low	≈zero		medium	medium	≈zero	
Iron	≈zero	≈zero	low		low	low	high	

NA: Information not available, because no useful EDS spectra were collected.

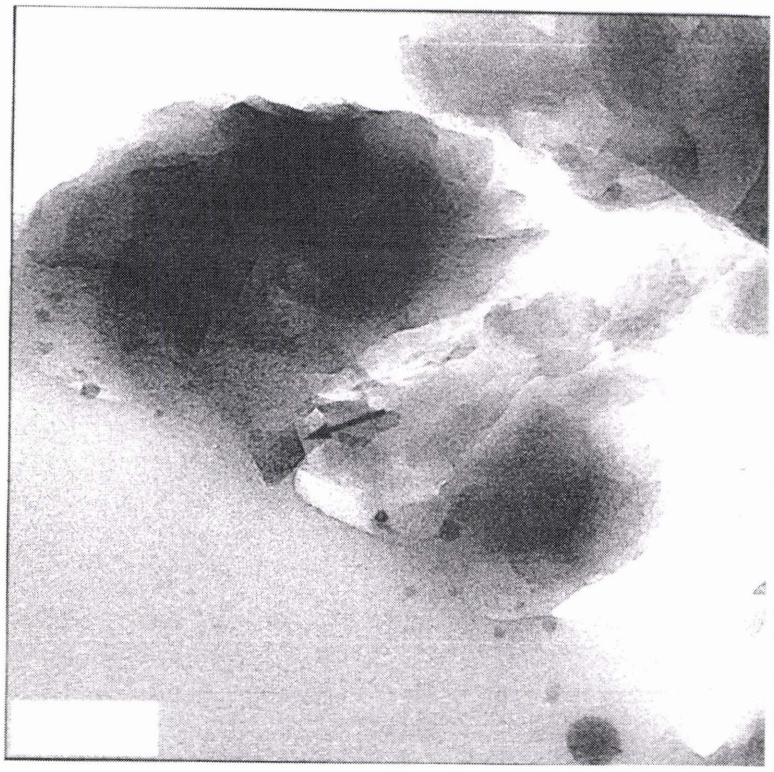

Figure 25. TEM micrograph of an ultramicrotome thin section of a bituminous bright char showing 10-20 nm-diameter inorganic inclusions.

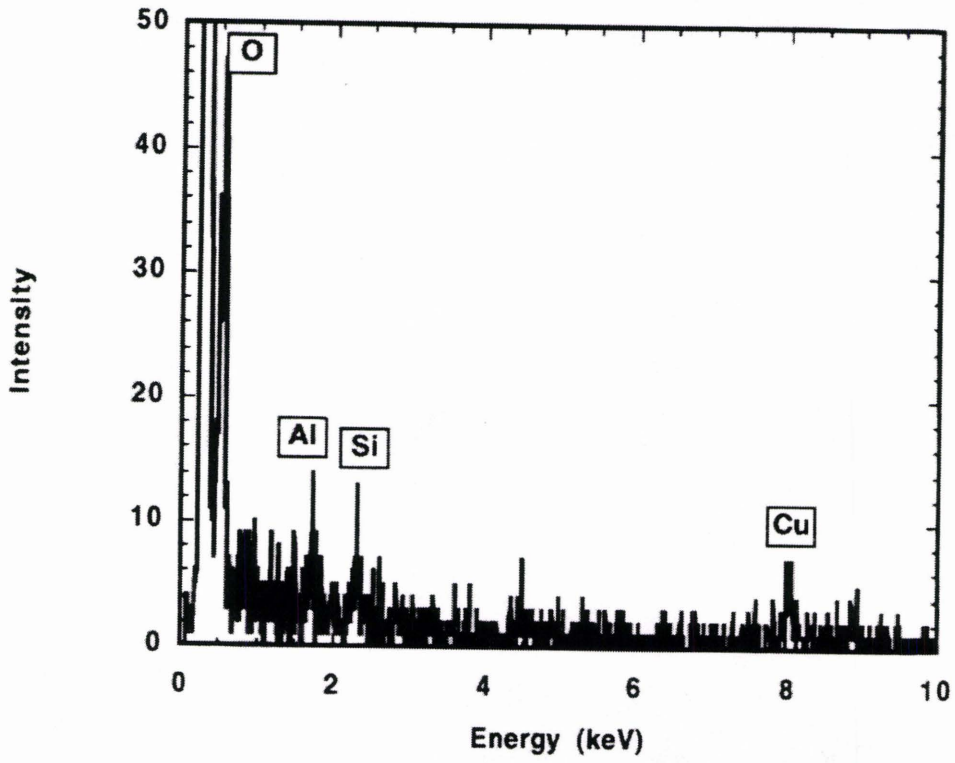

Figure 26. Energy dispersive spectrum showing regular elemental composition for bituminous bright char matrices.

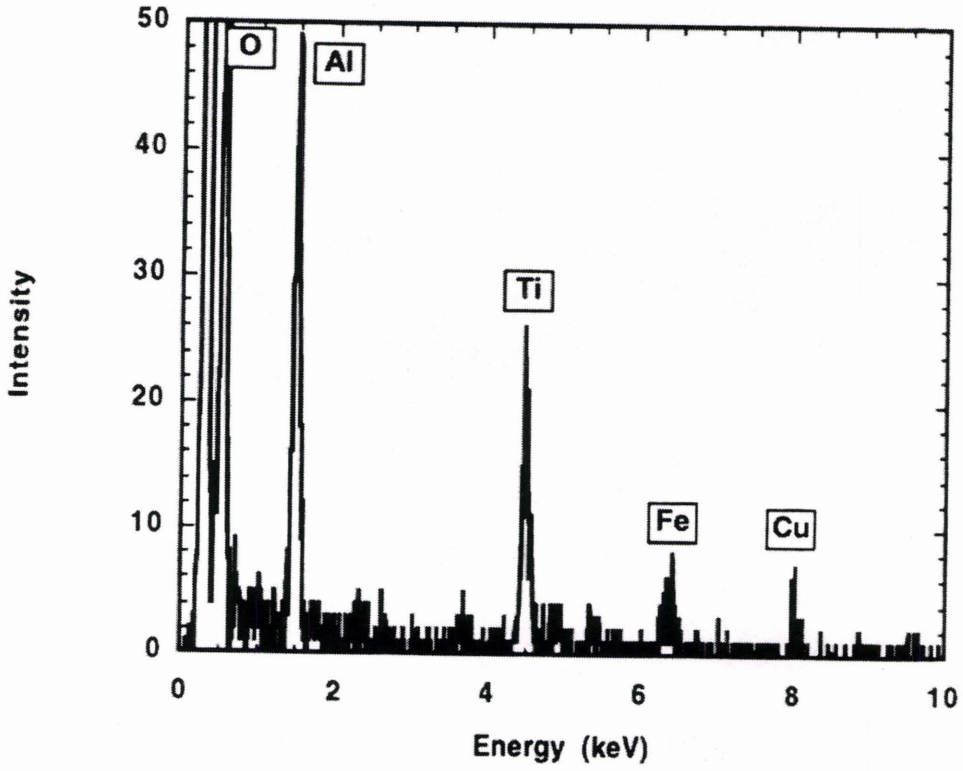

Figure 27. Elemental compsition for the nanometer-scale inclusions in the bituminous bright char shown in Figure 25.

Inorganic components observed in the bituminous dull char are about 10-30 nm in diameter. The EDS spectra for all of the nanometer-scale components show strong energy dispersive peak intensities for titanium, and lower intensities for calcium, iron, and aluminum. Silicon and sulfur are enriched in some inclusions. A grouping of three interconnected particles contains abundant titanium, calcium, iron, and aluminum (Figure 28 and 29). Each individual grain is between 10 and 15 nm in diameter. A second cluster was examined in another char particle. It had similar chemistry. All of the char matrices examined have high energy dispersive peak intensities for carbon and oxygen (Figure 30). EDS spectra reveal low X-ray intensities for sulfur, silicon, calcium, and aluminum in some char matrices.

Wyodak Subbituminous Char

The subbituminous bright char contains inorganic inclusions approximately 10 to 20 nm in diameter (Figure 31). These inclusions are uniformly dispersed in most char particles examined. Iron is enriched in all of the inorganic components observed (Figure 32). Calcium is also present in many of the included grains. Low intensity energy dispersive peaks were obtained for sulfur, aluminum, and magnesium which also may be concentrated in most of the nanometer-scale inclusions. Char matrices of this sample are composed of mostly carbon and oxygen, as is expected. Relatively minor peaks in EDS

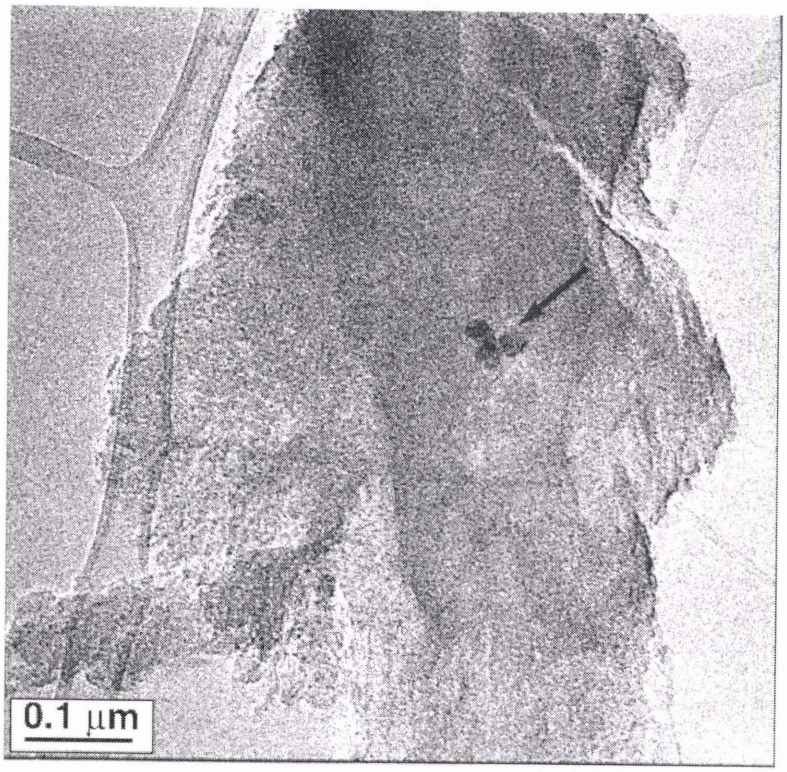

Figure 28. TEM photograph of a bituminous dull char particle containing a cluster of nanometer-scale inorgaic inclusions.

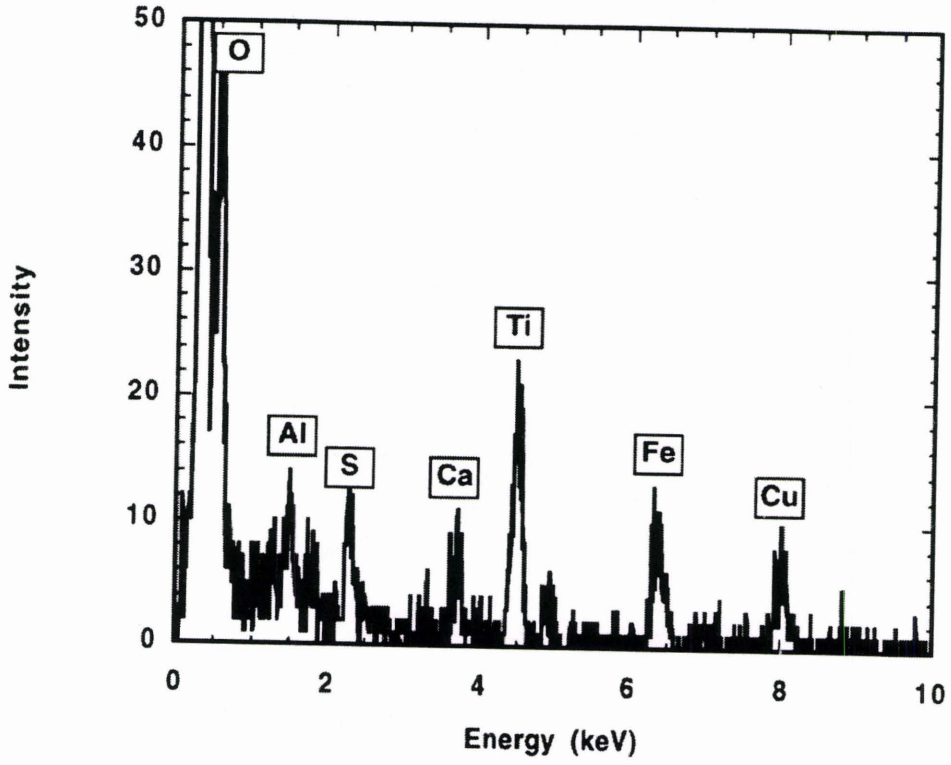

Figure 29. Elemental composition for the cluster of particles shown in the bituminous dull char in Figure 28.

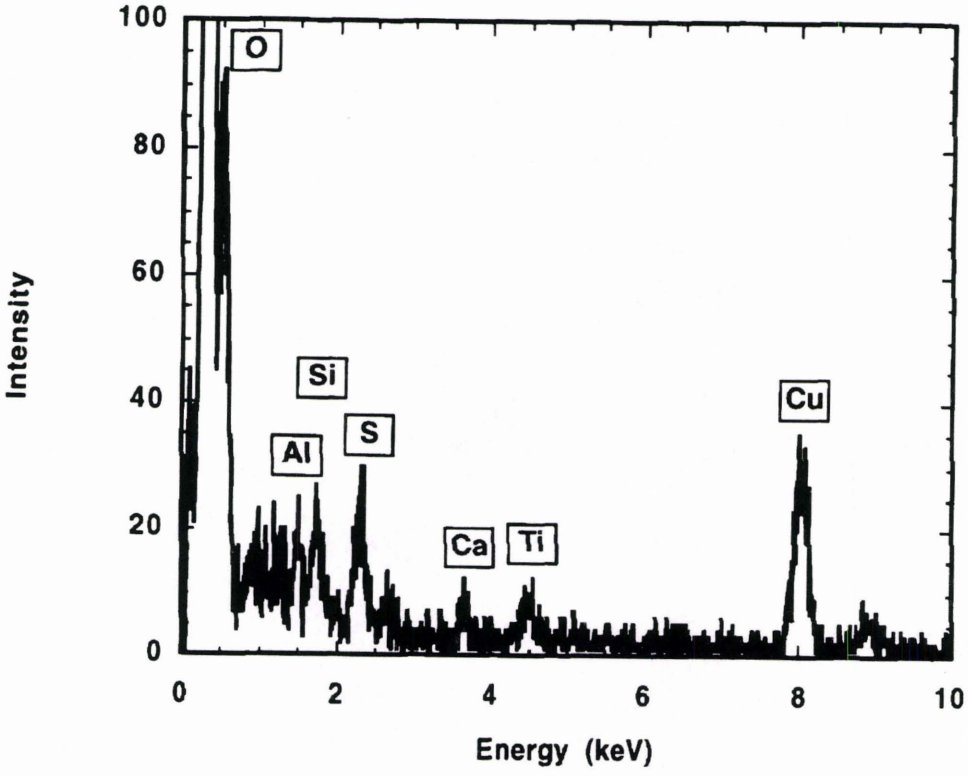

Figure 30. Energy dispersive spectrum showing regular elemental composition for bituminous dull char matrices.

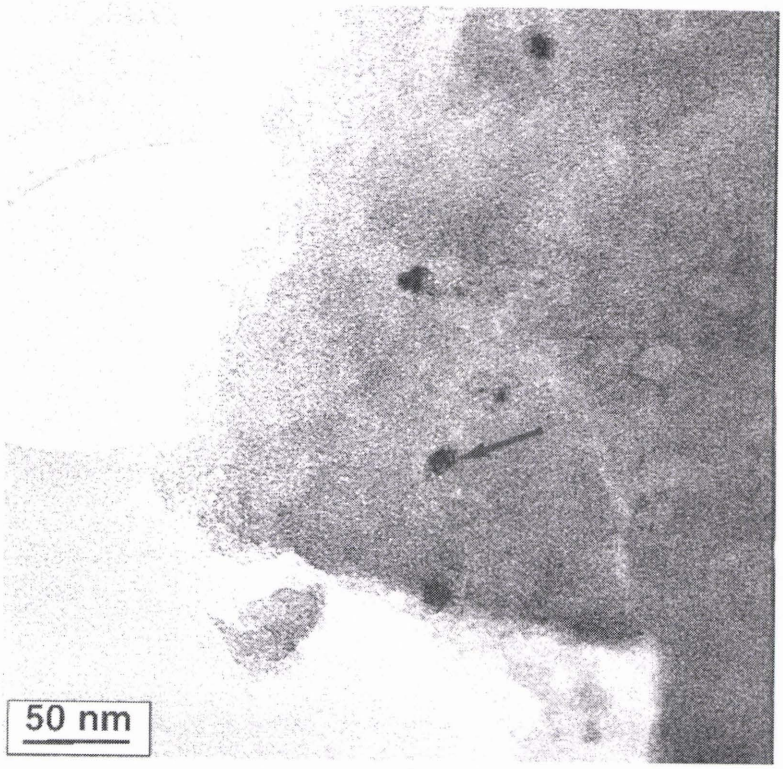

Figure 31. TEM photograph of a subbituminous bright char particle containing nanometer-scale inorganic particles.

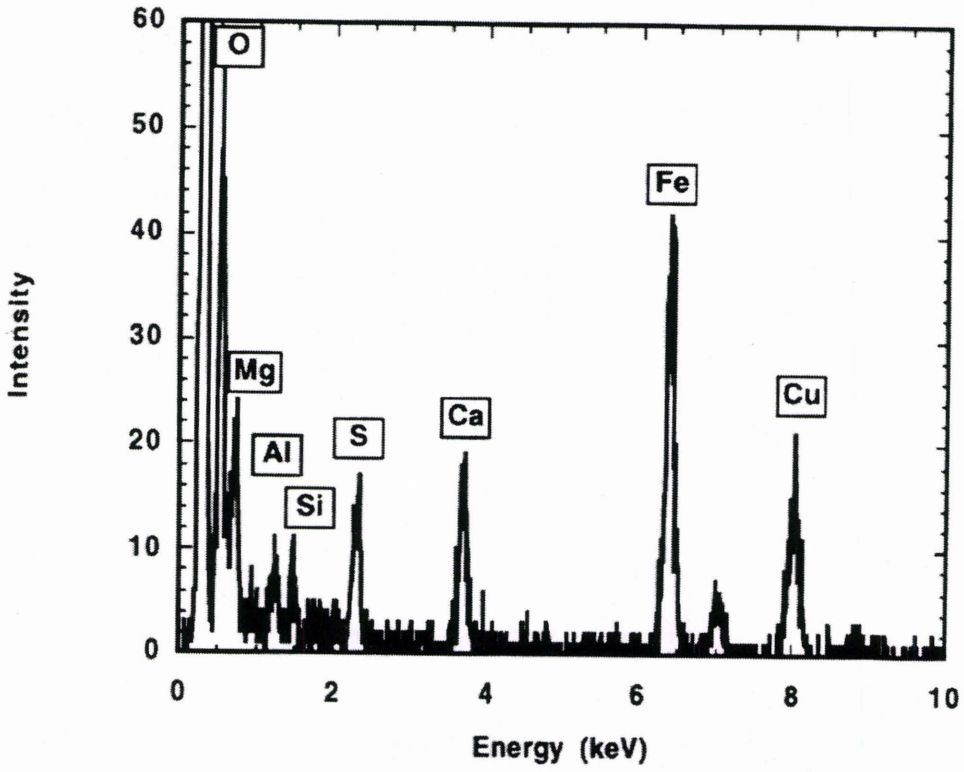

Figure 32. Elemental composition for the nanometer-scale inclusions in the subbituminous bright char shown in Figure 31.

spectra reveal low concentrations of sulfur, calcium, magnesium, aluminum, and sometimes iron (Figure 33).

Few char particles were determined to contain nanometer-scale inorganic inclusions in the subbituminous dull char. Carbon, sulfur, and calcium are common elements in the char matrices of this sample. Small inorganic inclusions approximately 15 to 25 nm in diameter provide EDS spectra with intense iron peaks. Inorganic components >50 nm give relatively intense calcium peaks. Sulfur, magnesium, and aluminum peaks are also present on EDS spectra of inorganic inclusions and char matrices.

Charform Abundance

Scanning electron microscopy was used at the UND-EERC to determine char morphologies produced by partial combustion of bituminous and subbituminous lithotypes. Rectangular blocks used to cut thin sections for the TEM were embedded in resin. These plugs were left overnight to cure, and then cut in half to produce cross sectional areas. The surface of each plug was polished and carbon coated. The scanning electron microscope (SEM) was used in back-scatter electron imaging mode, as opposed to secondary electron imaging mode. In back-scatter electron imaging, incident electrons are scanned across a specimen and are elastically scattered or reflected. The back-scattering coefficient is dependent on specimen atomic number and provides compositional contrast (Gopinath, 1974). Particles of high atomic number

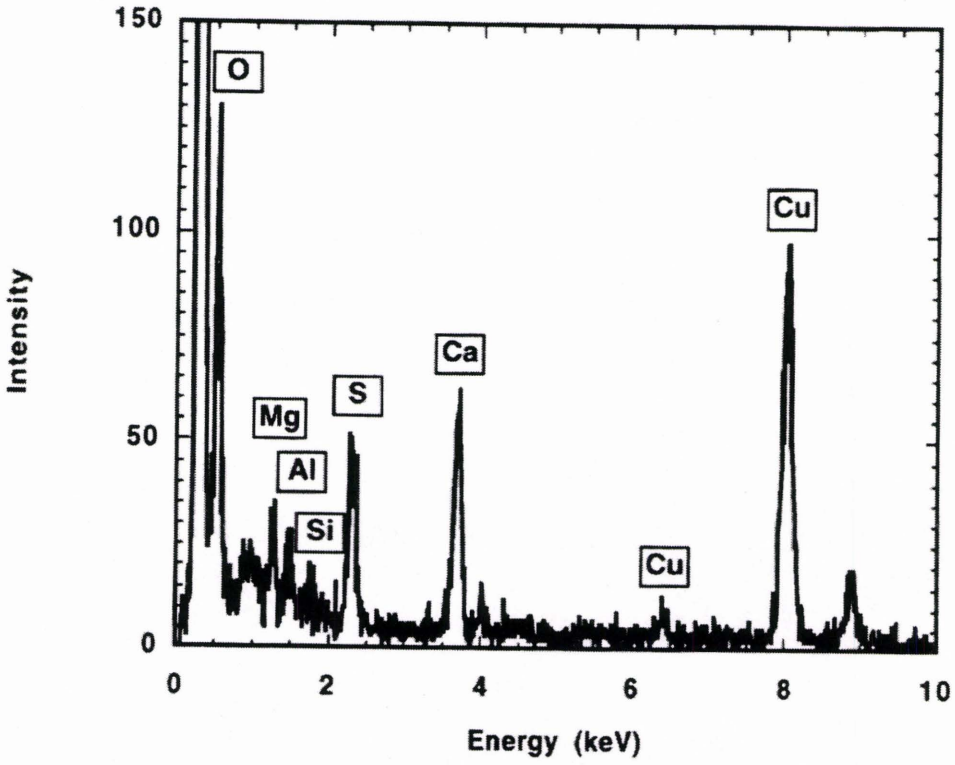

Figure 33. Energy dispersive spectrum showing regular elemental composition for subbituminous bright char matrices. Correction: The small Cu peak located to the left of the larger Cu peak is an Fe peak.

included within a specimen appear bright in back-scatter electron imaging, whereas material composed of lower atomic number elements will appear darker. Secondary electron imaging determines specimen topography. Secondary electrons have relatively low energies, and because of this, can be distinguished from back-scattered electrons by the electron collector in the SEM.

The rectangular blocks embedded in each plug were separated into fields in the SEM. A digital camera collected scanning electron micrographs for each field. These were then printed and assembled, replicating each field on a much larger scale. Areas of each char particle were digitized to determine abundance of the different charforms produced by bright and dull lithotypes.

Reactivity

Cenosphere and honeycomb charforms are generally categorized reactive, whereas solid charforms are considered inert. The term 'semi-reactive' is also used to describe charforms that have reactive and inert characteristics. For the char produced by bituminous lithotypes, reactive charforms include thin-walled and thick-walled cenosphere, thin-walled cenosphere containing inert char, thin-walled honeycomb, and thin-walled honeycomb containing inert char. Thick-walled honeycomb and thick-walled honeycomb containing inert char are classed semi-reactive. The inert charforms are solid/inert particle and solid/inert particle containing pores. For char produced by subbituminous lithotypes, the reactive charforms are thin-walled and thick-walled honeycomb and mixed thin-

/thick-walled honeycomb. The inert charforms include mixed solid/honeycomb, solid containing cracks and cavities, solid, and fragmented solid. The degree of reactivity of a given char particle governs rate of burnout and may govern the degree of shedding or coalescence of ash that appears on the surface of the particle during combustion. Figure 34 shows the abundance of the different charforms. The bright lithotypes of both coals produced more reactive than inert charforms. The dull lithotypes of both coals did not produce more inert charforms than reactive, but did produce more inert charforms than their related bright lithotypes. The bituminous dull lithotype produced significantly more semi-reactive charforms than the bituminous bright lithotype. These results clearly show that lithotype reactivity determines char formation in a PFBR.

Charforms Produced by Pittsburgh #8 Bituminous Lithotypes

The charforms produced by bituminous bright lithotypes in order of decreasing reactivity are thin-walled cenosphere, thick-walled cenosphere, thin-walled honeycomb, thin-walled honeycomb containing inert char, thick-walled honeycomb, and solid/inert particle. A thin-walled cenosphere char particle is shown in Figure 35. Abundance of the different charforms are as follows: thin-walled cenosphere, 2.5%; thick-walled cenosphere, 0.2%; thin-walled honeycomb, 66.9%; thin-walled honeycomb containing inert char, 26.9%; thick-walled honeycomb, 2.9%; and solid/inert particle, 0.6% (Table 10). Reactive

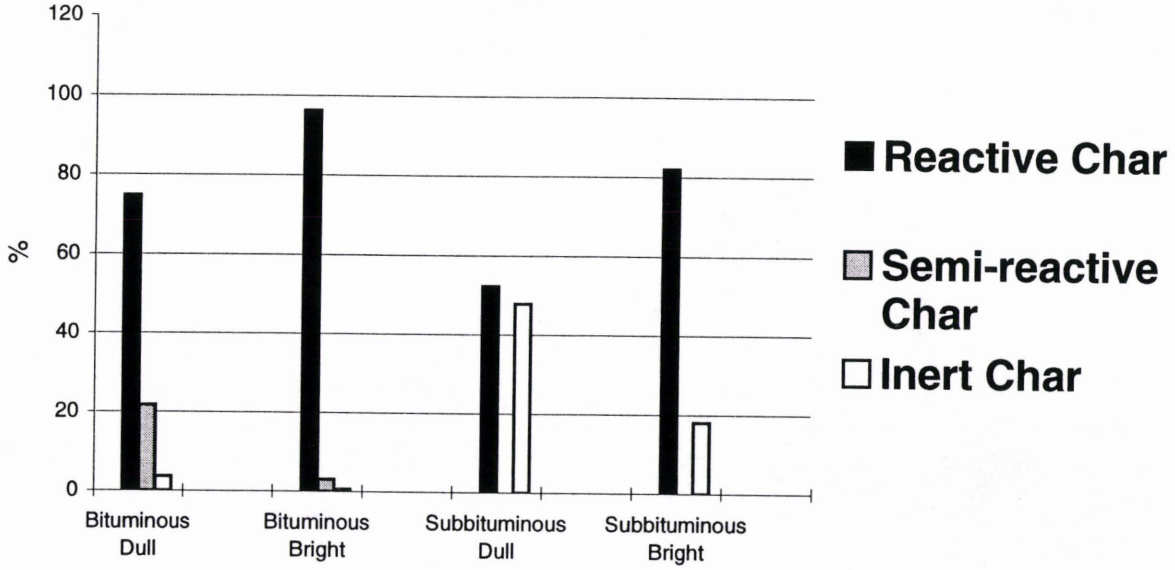

Figure 34. Reactive, semi-reactive, and inert charform abundance.

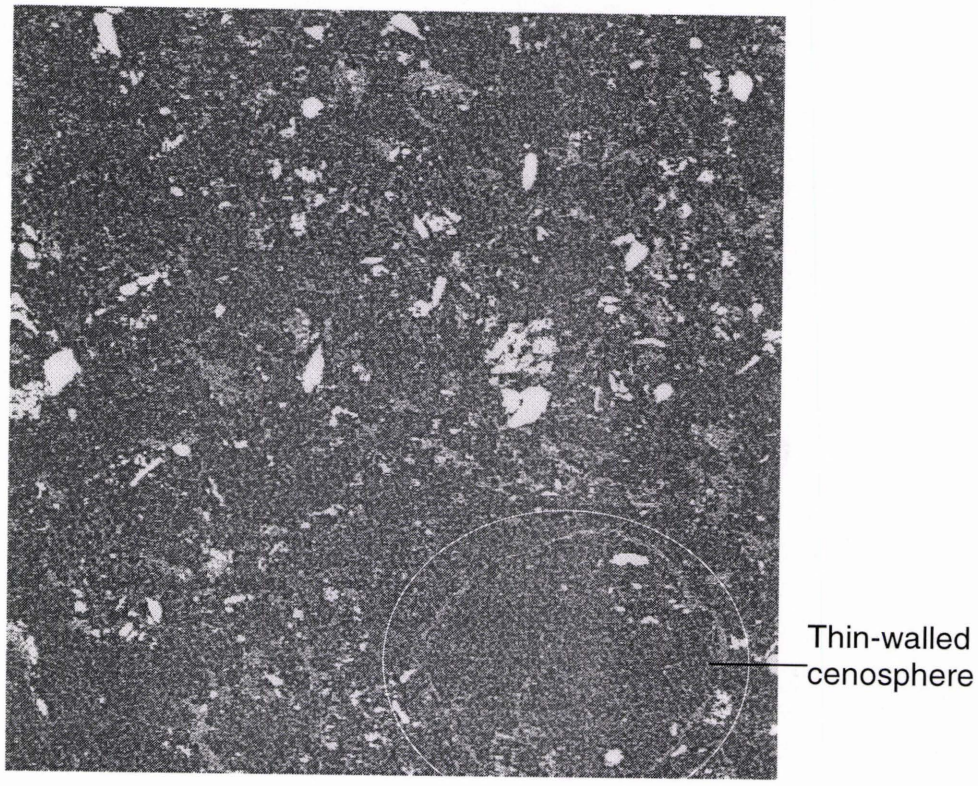

Figure 35. SEM micrograph of a thin-walled cenosphere char particle produced by the bituminous bright lithotype. The bright material is ash.

Table 10. Image analysis data for char produced by the Pittsburgh #8 bituminous bright lithotye.

	total area (square microns)	% of total char
Thin-walled cenosphere	428793	2.5
Thin-walled honeycomb	1E+07	67.0
Thin-walled honeycomb containing inert components	5E+06	26.9
Thick-walled cenosphere	25534	0.2
Thick-walled honeycomb	487968	2.9
Solid, inert particle	99598	0.6
Reactive char	15454327	96.3
Semi-reactive char	487968	3.0
Inert char	99598	0.6

charforms make up 96.3% of the total char, whereas semi-reactive and inert charforms constitute 3.0% and 0.6%, respectively.

Charforms produced by the bituminous dull lithotype are the same as for the charforms produced by the bituminous bright lithotype with the addition of thin-walled cenosphere containing inert char, thick-walled honeycomb containing inert char, and solid/inert particle containing pores. Figures 36, 37 and 38 show thin- and thick-walled honeycomb structures, and a solid, inert char particle. Abundance in order of decreasing reactivity for these charforms are: thin-walled cenosphere, 3.4%; thick-walled cenosphere, 6.2%; thin-walled cenosphere containing inert char, 1.5%; thin-walled honeycomb, 41.2%; thin-walled honeycomb containing inert char, 20.6%; thick-walled honeycomb containing inert char, 3.5%; thick-walled honeycomb, 20.4%; solid/inert particle containing pores, 0.2%; and solid/inert particle, 3.2% (Table 11). Reactive, semi-reactive, and inert charforms comprise 74.7%, 21.7%, and 3.6% of the total char.

Charforms Produced by Wyodak Subbituminous Lithotypes

The abundance of charforms produced by subbituminous bright lithotype in order of decreasing reactivity include: thin-walled honeycomb, 48.3%; vesicular, 10.3%; thick-walled honeycomb, 13.8%; mixed, thin-/thick-walled honeycomb, 9.0%; mixed, solid/honeycomb, 7.8%; solid containing cracks and cavities, 7.3%; solid, 1.1%; and fragmented solid, 0.3% (Table 12). Reactive charforms comprise 82% of the total char produced by the subbituminous bright

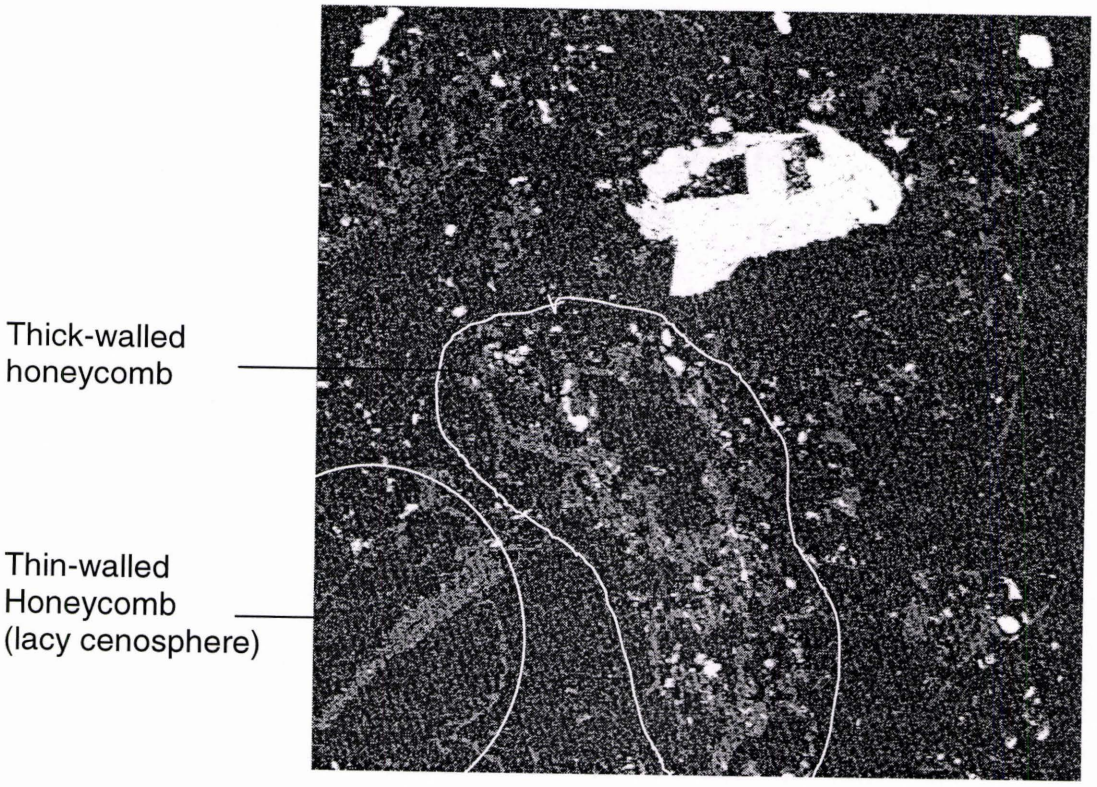

Figure 36. SEM micrograph of thin- and thick-walled honeycomb (lacy cenosphere) charforms produced by the bituminous dull lithotype. The bright materal is ash.

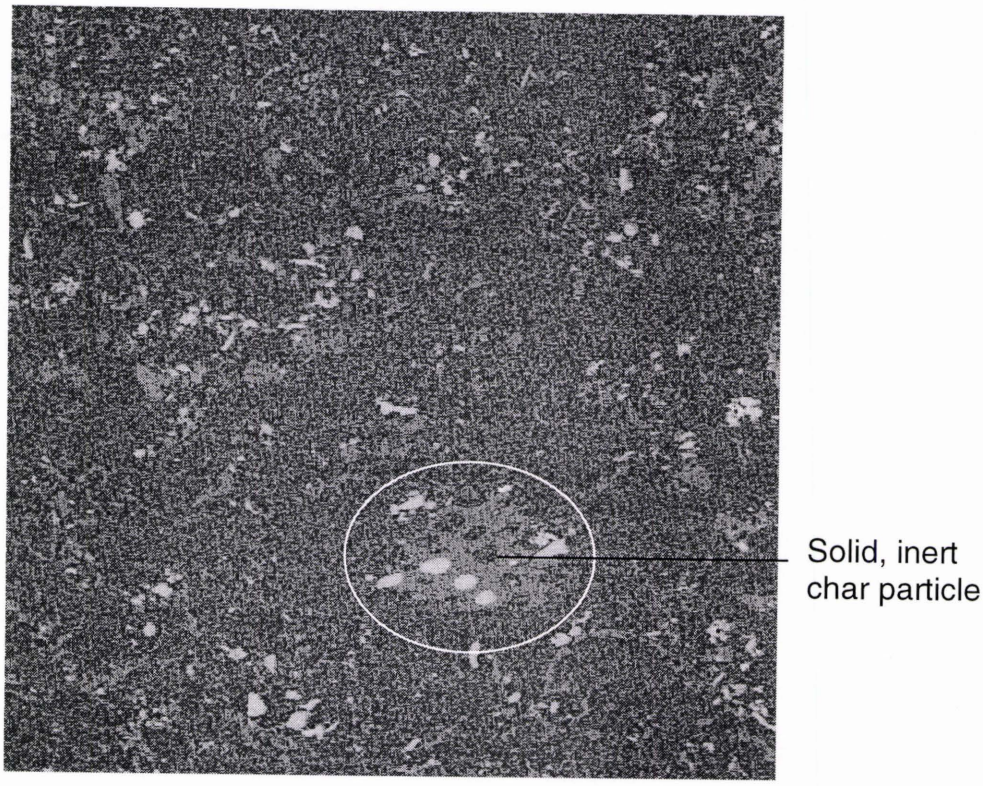

Figure 37. SEM micrograph of a solid, inert char particle produced by the bituminous dull lithotype. The bright material is ash.

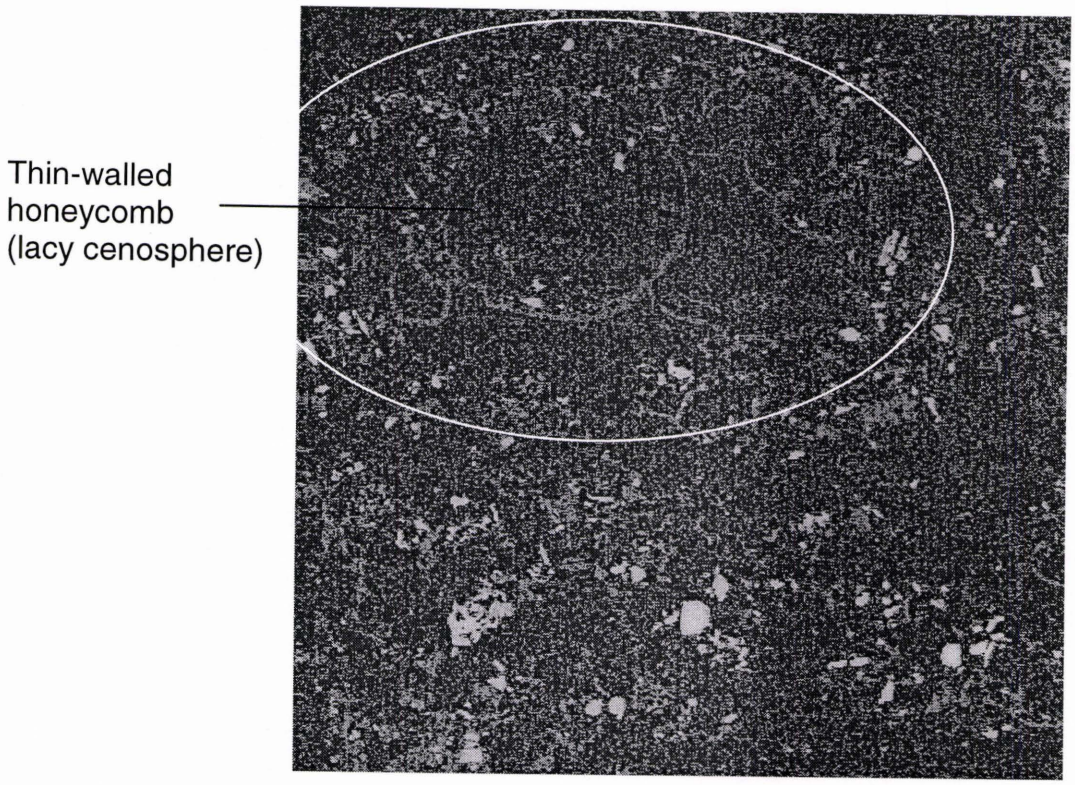

Figure 38. SEM micrograph of a thin-walled honeycomb (lacy cenosphere) charform produced by the bituminous dull lithotype. The bright material is ash.

Table 11. Image analysis data for char produced by the Pittsburgh #8 bituminous dull lithotye.

	total area (square microns)	% of total char
Thin-walled cenosphere	393820	3.4
Thin-walled honeycomb	5E+06	41.2
Thin-walled cenosphere containing inert components	171422	1.5
Thin-walled honeycomb containing inert component	2E+06	20.6
Thick-walled cenosphere	721819	6.2
Thick-walled honeycomb	2E+06	20.4
Thick-walled honeycomb containing inert components	405818	3.5
Solid, inert particle	370891	3.2
Solid with few pores	24762	0.2
Reactive char	8287061	74.7
Semi-reactive char	2405818	21.7
Inert char	395653	3.6

Table 12. Image analysis data for char produced by the Wyodak subbituminous bright lithotye.

	total area (square microns)	% of total char
Thin-walled Honeycomb	3E+06	48.3
Vesicular	731614	10.3
Thick-walled Honeycomb	984726	13.8
Mixed, thin-walled/thick-walled	637623	9.0
Mixed, solid and honeycomb	552831	7.8
Solid with cracks and cavities	521774	7.3
Dense	79345	1.1
Solid, fragmented	20087	0.3
Reactive char	5353963	82.0
Inert char	1174037	18.0

lithotype. Figure 39 shows some of the char structures in the subbituminous bright lithotype.

The charforms produced by the dull lithotype differ significantly from those produced by the bright. Thick-walled honeycomb charforms are segregated into three categories; parallel fragmented, parallel layered and parallel elongate pores. The mixed charforms observed in the char produced by the bright lithotype are absent in this char, as is the vesicular charform. In order of decreasing reactivity, the abundance of the different charforms are as follows: thin-walled honeycomb, 18.4%; thick-walled honeycomb, 33.7%; solid containing cracks and cavities, 21.3%; fragmented solid, 13.4%; and solid, 13.2% (Table13). Fifty two percent of the total char comprise reactive charforms. Chartypes produced by the subbituminous dull lithotype can be seen in Figure 40.

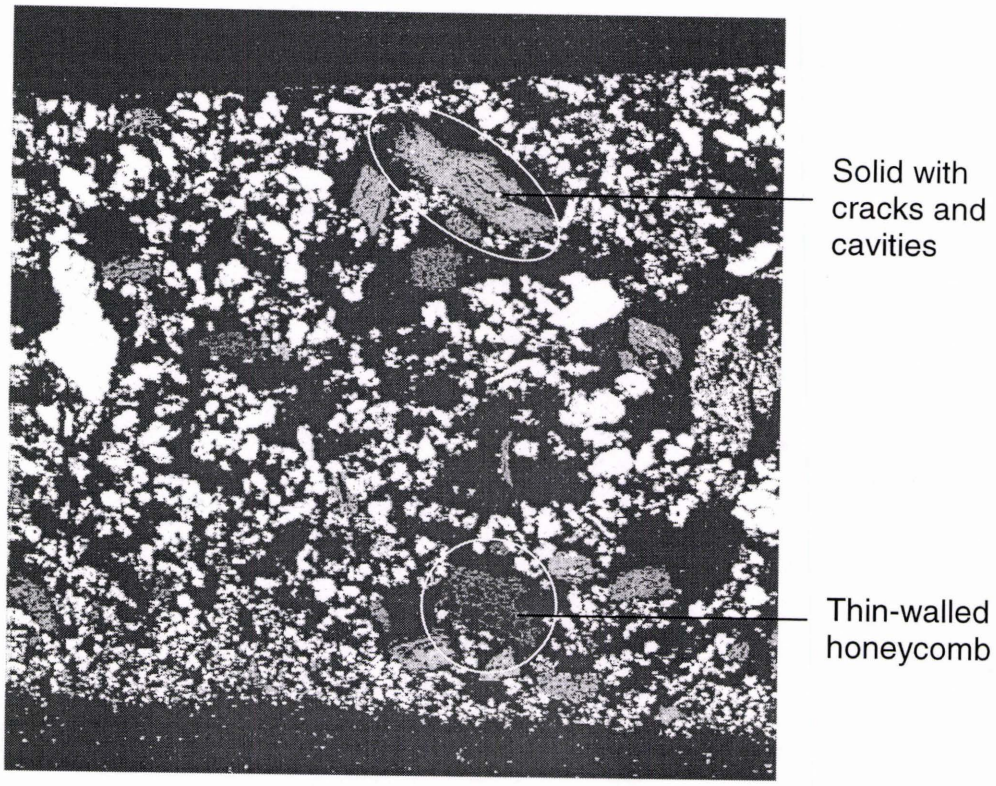

Figure 39. SEM micrograph of a solid char with cracks and cavities, and a thin-walled honeycomb charform produced by the subbituminous dull lithotype. The bright material is ash.

Table 13. Image analysis data for char produced by the Wyodak subbituminous dull lithotye.

	total area (square microns)	% of total char
Thin-walled Honeycomb	343016	18.4
Thick-walled Honeycomb		
parallel fragmented	356169	19.1
parallel layered	69129	3.7
parallel elongate pores	202614	10.9
Solid with cracks and cavities	396141	21.3
Solid, fragmented	248795	13.4
Dense	245911	13.2
Mixed, solid and honeycomb	NA	
Vesicular	NA	
Mixed, thin-walled/thick-walled	NA	
Reactive char	970928	52.2
Inert char	890847	47.8

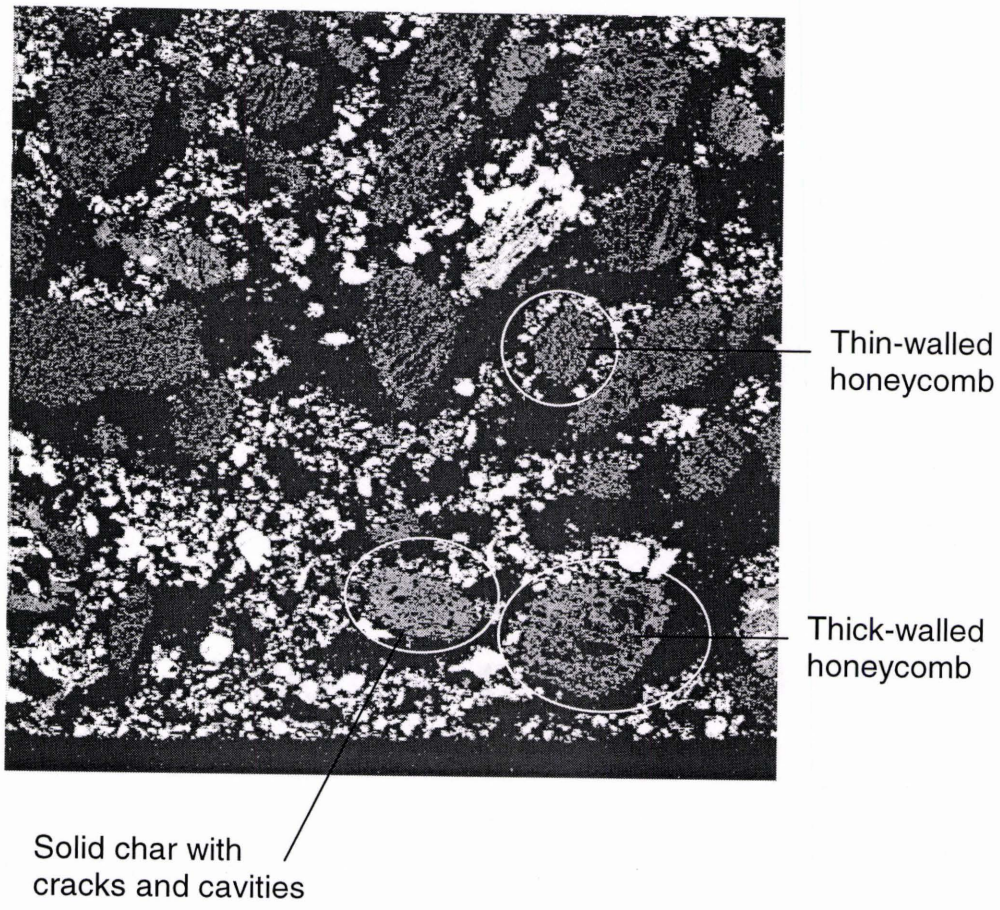

Figure 40. SEM micrograph of thin- and thick-walled honeycomb charforms and a solid char with cracks and cavities produced by the subbituminous bright lithotype. The bright material is ash.

CHAPTER IV

CONCLUSIONS AND DISCUSSION

Four main conclusions arise from the present research: (1) coal lithotypes control char morphology; (2) coal rank controls char formation; (3) nanometer-scale inclusions are present in Wyodak subbituminous bright coal and char produced from pressurized fluidized-bed combustion of Pittsburgh #8 and Wyodak bright and dull coals; and (4) coal lithotypes have very little influence on the formation of fine ash in a pressurized fluidized-bed combustion system. Previous research shows that the different macerals strongly affect how a coal burns, while this research shows the importance of coal lithotypes, assemblage of different macerals, on coal combustion, and on char and ash formation. Figure 41 summarizes the different charforms produced by partial combustion of bituminous and subbituminous bright and dull coal lithotypes in a pressurized fluidized-bed reactor.

Importance of Coal Lithotypes in Coal Combustion

Coal lithotypes are composed of characteristic assemblages of macerals that determine the reactivity of char. Bright lithotypes contain more reactive, vitrinite group macerals, and form reactive or porous charforms after partial combustion. Dull lithotypes contain less reactive, inertinite macerals and form more inert or solid charforms than the bright lithotypes. Ash particles that appear

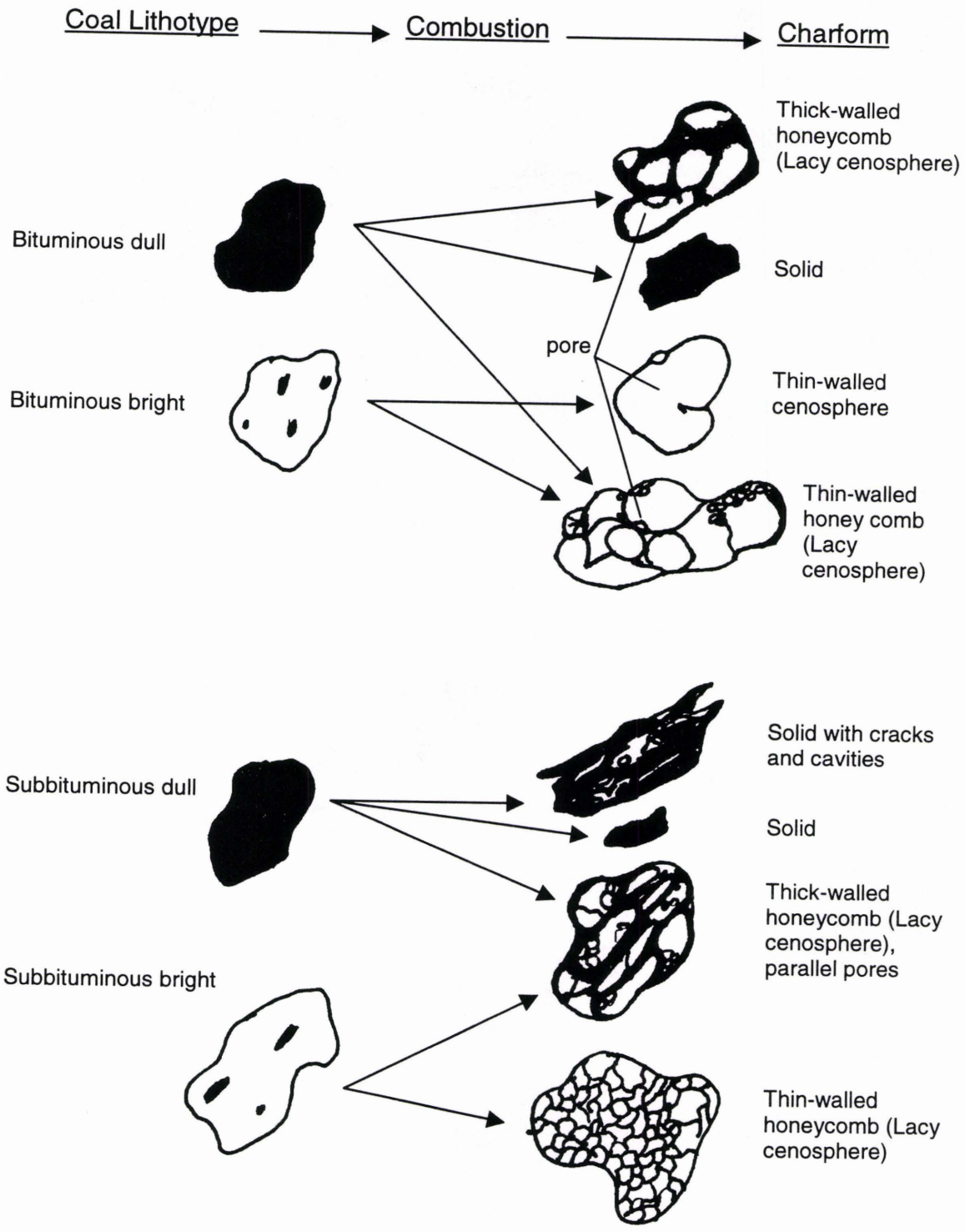

Figure 41. Bituminous and subbituminous bright and dull coal lithotypes and their associated charforms after partial combustion in a pressurized fluidized-bed reactor.

on the porous char formed by combustion of bright lithotypes may be contained within the pores, which may then coalesce to form larger ash particles as combustion proceeds. Ash particles that form on the surface of solid or dense charforms may shed at a rate faster than burnout of the char producing a fine and sticky ash that is difficult to remove from high temperature filters. An alternative model relating to char and ash evolution during coal combustion is that porous char burns in constant-diameter mode until the char particles and included ash grains burst into many small fragments while dense char burns in constant density or mixed modes shedding ash as it burns (Baxter, 1992). If this is correct, ash size is not related to char reactivity in a pressurized fluidized-bed combustion system. Lithotypes are defined by their maceral content and to some degree, the physical and chemical properties of included mineral components. Therefore, lithotype reactivity may be governed not only by maceral content, but also by inorganic content that may contribute to differences in physical and chemical properties of the ash.

Importance of Coal Rank in Coal Combustion

This study reveals that coal rank also strongly influences the morphology of char particles during combustion. Char cenosphere particles are produced only by the bituminous coal lithotypes. Honeycomb structures are produced by both bituminous and subbituminous coal lithotypes, but have very different appearances when examined with a scanning electron microscope. It is evident that the char fabricated by partial combustion of bituminous coal lithotypes

experiences a greater degree of thermal plasticity than the char produced by the subbituminous coal lithotypes. To the contrary, previous studies show that low rank coals produce reactive charforms and high rank coals produce more inert charforms. Generally, low rank coal contains a higher percentage of volatile matter or aliphatic hydrocarbons that are released as gas in combustion. If the particles experience thermal plasticity and pyrolysis occurs, the gas pressure inside the char produces a balloon or umbrella, thus forming a cenosphere charform. High rank coal commonly contains less volatile matter due to higher degree of coalification, thus inert or dense char particles form during combustion. Other studies show that loose physical structure of low rank coal permits combustion gases to penetrate into the particles promoting internal and external burning (mixed burning mode) that produce honeycomb or lacy cenosphere charforms. Oxygen cannot facilitate internal burning in high rank coal particles, because of longer coalification, hence a tight physical structure.

Importance of Nanometer-Scale Inorganic Inclusions in Coal Combustion

Nanometer-diameter particles occurring in coal may have a direct impact on the formation of fine ash during combustion. It is necessary to determine their abundance and identity in different parts of coal in order to gain useful information about their effect in the combustion process. Inorganic nanometer-scale inclusions are present in char produced by bright and dull lithotypes separated from bituminous and subbituminous coal. They are not extremely

abundant and are not disseminated in the char particles, but occur as isolated groups. Nanometer-scale inclusions are present in the subbituminous bright lithotype, but their identity is unknown. They may be inorganic components precipitated in sub-micron pores present in some macerals, or within organic molecular cages occurring in certain coal lithotypes. To the contrary, they may also be mesophase particles that form as a result of heating vitrinite macerals. Incident electrons emitted in the TEM may heat the sample to the point where mesophase spheres form. Further examination is necessary to determine whether the temperatures reached in the TEM are appropriate for the formation of mesophase spheres.

Effect of Coal Lithotypes on Fine Ash Formation

Although the present research shows that coal lithotypes play a minor role in the formation of fine ash in pressurized fluidized-bed combustion systems, they may be significant in conventional coal combustion, such as pulverized fuel combustion. Fragmentation of coal, char, and ash particles in a fluidized-bed combustion system is greater than in pulverized fuel combustion. If coal particles evolve without fragmentation in pulverized combustion, vesicular charforms may, indeed prevent the formation of fine and sticky ash, whereas dense charforms will produce fine and sticky ash. This, of course, requires additional research. There is some evidence that organically-bound inorganic elements are more abundant in the subbituminous coal, which may vaporize

during combustion, and then condense to form small ash particles. This is in agreement with previous studies.

REFERENCES CITED

Alvarez, Diego; Borrego, Angeles G.; and Menendez, Rosa, 1997. Unbiased Methods for the Morphological Description of Char Structures. Fuel, vol. 76, p. 1241-1248.

Annual Book of ASTM Standards, 1995. Gaseous Fuels: Coal and Coke, D 121-94, Standard Terminology of Coal and Coke, p. 137-147.

Bailey, Philip S. and Bailey, Christina A., 1995. Organic Chemistry, 5th Edition. Englewood Cliffs, New Jersey: Prentice-Hall, 560 p.

Baum, Rudy, 1997. Bowl-shaped PAH has C_{60}-like Reactivity. Chemical and Engineering News, December 1, p. 28.

Baxter, Larry L., 1992. Char Fragmentation and Fly Ash Formation During Pulverized-Coal Combustion. Combustion and Flame, vol. 90, p. 174-184.

Chircop, Jeanne, 1996. Facts About Coal. Washington, DC: National Mining Association, 84 p.

Chirone, R.; Massimilla, L.; and Salatino, P., 1991. Comminution of Carbons in Fluidized Bed Combustion. Prog. Energy Combust. Sci., vol. 17, p. 297-326.

Chirone, R.; Massimilla, L.; and Salatino, P., 1989. Secondary Fragmentation of Char Particles during Combustion in a Fluidized Bed. Combustion and Flame, vol. 77, p. 79-80.

Chyi, L.L.; Barnett, R.G.; Burford, A.E; Quick, T.J.; and Gray, R.J., 1987. Coalification Patterns of the Pittsburgh Coal: Their Origin and Bearing on Hydrocarbon Maturation. International Journal of Coal Geology, vol. 7, p. 69-83.

Cross, A.T., 1971. The Geology of the Pittsburgh Coal. West Virginia Geological and Economic Survey, Report of Investigations, No. 10, p. 32-99.

DOE, 1981. Economic Evaluation of Alternative Solutions to Decrease Boiler Ash Fouling. DOE/FC-102320-T1 p.1.

Damberger, Heinz H., 1974. Coalification Patterns of Pennsylvanian Coal basins of the Eastern United States. In: Russell R. Dutcher, Peter A. Hacquebard, James M. Schopf, and Jack A. Simon (Editors), Carbonaceous Materials as Indicators of Metamorphism. The Geological Society of America, Special Paper 153, Boulder, Co., p. 53-72.

Dockter, Bruce A.; Erickson, Thomas A.; Henderson, Ann K.; Hurley, John P.; Kuhnel, Vit; Nowok, Jan W.; Swanson, Michael L.; and Tomforde, Chad G., 1997. Hot-Gas Filter Ash Characterization Project. Quarterly Technical Progress Report, August through October 1996, Contract No. RP3910-01. University of North Dakota-Energy and Environmental Research Center.

Edmunds, William E., 1993. Pennsylvania Description of Seams. In: Keystone Coal Industry Manual. Chicago: Maclean Hunter Publishing Company, p. 127 - S-138.

Francis, Wilfrid, 1961. Coal, Its Formation and Composition, 2nd Edition. London: Edward Arnold Ltd., 806 p.

Friel, John J.; Mehta, Sudhir; Mitchell, Gareth D.; and Karpinski, John M., 1980. Direct Observation of the Mesophase in Coal. Fuel, vol. 59, p. 610-616.

Gerencher, Joseph Jr., 1983. A Multivariate Study of the Interrelationships among Selected Variables of the Organic Fraction of Samples of United States' Coals. In: Alan Davis (Editor), A Data Base for the Analysis of compositional Characteristics of Coal Seams and Macerals, Final Report-Part 2. Pennsylvania State University, University Park, PA. for DOE/PC/30013-F2, 613 p.

Given, Peter H., 1984. An Essay on the Organic Geochemistry of Coal. In: M.L. Gorbaty, J.F. Larson, and I. Wender (Editors), Coal Science, vol. 3. Academic Press, Inc., p. 63-341.

Glass, Gary B., 1976. Wyoming Coal Deposits. Symposium on the Geology of Rocky Mountain Coal, p. 73-84.

Gopinath, A., 1974. The Emissive Mode. In: D.B Holt, M.D. Muir, P.R. Grant, and I.M. Boswarva (Editors), Quantitative Scanning Electron Microscopy. New York: Academic Press, p. 95-130.

Goss, James, 1996. Personal Communication. Eagle Butte Coal Mine, Gillette, Wyoming.

Groenewold, Gerald H.; Hemish, LeRoy A.; Cherry, John A.; Rehm, Bernd W.; Meyer, Gary N.; and Winczewski, Laramie M., 1979. Geology and Geohydrology of the Knife River Basin and Adjacent Areas of West-Central North Dakota. North Dakota Geological Survey, Report of Investigation No. 64, 402 p.

Hamilton, Lloyd H., 1980. Char Morphology and Behaviour of Australian Vitrinites of Various Ranks Pyrolysed at Various Heating Rates. Fuel, vol. 60, p. 909-913.

Harris, L. A. and Yust, C.S., 1981. The Ultrafine Structure of Coal Determined by Electron Microscopy. In: Martin L. Gorbaty and K. Ouchi (Editors), Coal Structure: Advances in Chemistry Series 192. Washington, DC: American Chemical Society, p. 133-155.

Harris, Lawrence A. and Yust, Charles S., 1976. Transmission Electron Microscope Observations of Porosity in Coal. Fuel, vol. 55, p. 233-236.

Helble, J.J. and Sarofim, A.F., 1989. Influence of Char Fragmentation on Ash Particle Size Distributions. Combustion and Flame, vol. 76, p. 183-196.

Hennig, G.R., 1962. Catalytic Oxidation of Graphite. Journal of Inorganic and Nuclear Chemistry, vol. 24, p. 1129-1137.

Hower, James C. and Esterle, John S., 1989. Coal Lithotype Analysis: Problems and Potential. Highlights, University of Kentucky, vol. 8, no. 4.

Hurley, John P., 1990. A Pilot-Scale Study of the Formation of Ash during Pulverized Low-Rank Coal Combustion. Pennsylvania State University, Doctoral Dissertation, 247 p.

Hurley, John P. and Schobert, Harold H., 1993. Ash Formation during Pulverized Subbituminous Coal Combustion. 2. Inorganic Transformations during Middle and Late Stages of Burnout. Energy and Fuels, vol. 7, 542-553.

Hurley, John P. and Schobert, Harold H., 1992. Ash Formation during Pulverized Subbituminouus Coal Combustion. 1. Characterization of

Coals, and Inorganic Transformations During Early Stages of Burnout. Energy and Fuels, vol. 6, p. 47-58.

International Committee for Coal Petrology (ICCP), 1971. International Handbook of Coal Petrography (Supplement 1), Centre National De La Recherche Scientifique, Paris.

Jones, R.B.; McCourt, C.B.; Morley, C.; and King, K., 1985. Maceral and Rank Influences on the Morphology of Coal Char. Fuel, vol. 64, p. 1460-1467.

Jones, R.B.; Morley, C.; and McCourt, C.B, 1985. Maceral Effects on the Morphology and Combustion of Coal Char. Proc. 1985 Int. Conference on Coal Science. Sydney: Pergamon Press, p. 669-672.

Karner, Frank R.; Zygarlicke, Christopher J.; Brekke, David W.; Steadman, Edward N.; and Benson, Steven A., 1994. New Analysis Techniques Help Control Boiler Fouling. Power Engineering, p. 35-38.

Kent, Bion H., 1986. Evolution of Thick Coal Deposits in the Powder River Basin, Northeastern Wyoming. In: Paul C. Lyons and Charles L. Rice (Editors), Paleoenvironmental and Tectonic Controls in Coal-Forming Basins in the United States. Geological Society of America Special Paper 210, p. 105-122.

Kleesattel, David, 1982. Petrology of the Beulah-Zap Lignite Bed, Sentinel Butte Formation (Paleocene) Mercer County, North Dakota. University of North Dakota, Thesis, 188 p.

Klein, Cornelis and Hurlbut, Cornelius S. Jr, 1993. Manual of Mineralogy, 21st Edition. New York : John Wiley & Sons, Inc., 681 p.

Kube, W.R.; Schobert, Harold H.; Benson, S.A; and Karner, F.R., 1984. The Structure and Reactions of Northern Great Plains Lignites. In: Harold H. Schobert (Editor), The Chemistry of Low-Rank Coals: American Chemical Society Symposium Series 264. Washington, D.C.: American Chemical Society, p. 39-51.

Lightman, P. and Street, P.J., 1967. Microscopical Examination of Heat Treated Pulverized Coal Particles. Fuel, vol. 47, p. 7-28.

McCollor, Donald P.; Sweeny, Philip G.; and Benson, Steven A., 1988. Coal/Char Reactivity. Final Technical Report for the Period April 1, 1987-March 31, 1988 Including the Quarterly Technical Progress Report for the

Period January through March 1988 Performed Under Cooperative Agreement No. DF-FC21-86MC10637. University of North Dakota-Energy and Environmental Research Center.

Pregermain, S., 1988. Rank and Maceral Effects on Coal Combustion Characteristics. Fuel Processing Technology, vol. 20, p. 297-306.

Sawyer, John; Bass, R.J.; Brown, N.R.; and Brown, J.J, 1990. Corrosion and Degradation of Ceramic Particulate Filters in Direct Coal-Fired Turbine Applications. Transactions of the American Society of Mechanical Engineers, p. 2-5.

Shibaoka, Michio, 1985. Microscopic Investigation of Unburnt Char in Fly Ash. Fuel, vol. 64, p. 263-269.

Shibaoka, M.; Thomas, C.G.; Young, B.C.; Oka, N.; Matsuoka, H.; Tamaru, K.; and Murayama, T., 1985. The Influence of Rank and Maceral Composition on Combustion of Pulverized Coal. Proc. 1985 Int. Conference of Coal Science. Sydney : Pergamon Press, p. 665-668.

Stach, E.; Mackowsky, M.-Th.; Teichmueller, M.; Taylor, G.H.; Chandra, D.; and Teichmueller, R., 1975. Stach's Textbook of Coal Petrology, 3rd Edition. Berlin: Gebruder Borntraeger, 535 p.

Stach, E.; Mackowsky, M.-Th.; Teichmueller, M.; Taylor, G.H.; Chandra, D.; and Teichmueller, R., 1982. Stach's Textbook of Coal Petrology, 4th Edition. Berlin: Gebruder Borntraeger, 535 p.

Stone, Ralph W., 1932. Geology and Mineral Resources of Greene County, Pennsylvania. Pennsylvania Geological Survey, 4th Series, 175 p.

Stopes, M.C., 1919. On the Four Visible Ingredients in Banded Bituminous Coal. Proceedings of the Royal Society, B, vol. 90, p. 470-487.

Stout, S.A. and Spackman, W., 1987. A Microscopic Investigation of Woody Tissues in Peats: Some Processes Active in the Peatification of Ligno-Cellulosic Cell Walls. International Journal of Coal Geology, vol. 8, p. 55-68.

Teichmueller, M. and Teichmueller, R., 1982. The Geological Basis of Coal Formation, translation by D.G. Murchison. In: E. Stach, M.-Th. Mackowsky, M. Teichmueller, G.H. Taylor, D. Chandra, and R.

Teichmueller, Stach's Textbook of Coal Petrology. Berlin: Gebruder Borntraeger, 535 p.

Teichmueller, Marlies and Teichmueller, Rolf, 1968. Geological Aspects of Coal Metamorphism. In: Duncan Murchison and T. Stanley Westoll (Editors), Coal and Coal-Bearing Strata. New York: American Elsevier Publishing Company, Inc., p. 233-267.

Teichmueller, M. and Teichmueller, R., 1967. Diagenisis of Coal (Coalification). In: Gunnar Larsen and George V. Chilingar (Editors), Developments in Sedimentology 8: Diagenesis in Sediments. New York: Elsevier Publishing Company, p. 391-416.

Teichmueller, M. and Teichmueller, R., 1966. Geological Causes of Coalification. In: Robert F. Gould (Editor), Coal Science: Advances in Chemistry Series 55. Washington, DC: American Chemical Society, p. 133-155.

Theissen, R. and Francis, W, 1929. Terminology in Coal Research. Fuel, vol. 8, No. 8, p. 385-405.

Van Krevelen, D.W., 1981. Coal: Typology, Chemistry, Physics and Constitution. In: Larry L. Anderson (Editor), Coal Science and Technology, vol. 3. New York: Elsevier Scientific Publishing Company, 514 p.

Zareie, Hadi; Oztas, Nursen; Gundogan, Mehtap, Piskin, Erhan; and Yurum, Yuda, 1996. Images of Demineralized Coal Surfaces by Scanning Tunnelling Microscopy. Fuel, vol. 75, p. 855-857.

Zheng, Yushou and Wang, Zhijun, 1996. Distribution and Burning Modes of Char Particles during Combustion. Fuel, vol. 75, p. 1434-1440.